IEEE Access
Multidisciplinary | Rapid Review | Open Access Journal

Received December 20, 2021, accepted February 15, 2022, date of publication February 17, 2022, date of current version March 2, 2022.

Digital Object Identifier 10.1109/ACCESS.2022.3152570

Stochastic Delay Cost Functions to Estimate Delay Propagation Under Uncertainty

JAN EVLER [1], MICHAEL SCHULTZ [1], HARTMUT FRICKE [1], AND ANDREW COOK [2]
[1]Institute of Logistics and Aviation, Technische Universität Dresden, 01069 Dresden, Germany
[2]College of Design, Creative and Digital Industries, University of Westminster, London W1B 2HW, U.K.

Corresponding author: Jan Evler (jan.evler@tu-dresden.de)

This work was supported in part by the German Federal Ministry of Economic Affairs and Climate Action (BMWK) within the LUFO-V Project OPsTIMAL under Agreement 20X1711M and in part by the SESAR Joint Undertaking through the European Union's Horizon 2020 Research and Innovation Program under Agreement 783287 (Engage KTN).

ABSTRACT We provide a mathematical formulation of flight-specific delay cost functions that enables a detailed tactical consideration of how a given flight delay will interact with all downstream constraints in the respective aircraft rotation. These functions are reformulated into stochastic delay cost functions to respect conditional probabilities and increasing uncertainty related to more distant operational constraints. Conditional probabilities are learned from historical operations data, such that typical delay propagation patterns can support the flight prioritization process as a part of tactical airline schedule recovery. A case study compares the impact of deterministic and stochastic cost functions on optimal recovery decisions during an airport constraint. We find that deterministic functions systematically overestimate potential disruption costs as well as optimal schedule recovery costs in high delay situations. Thus, an optimisation based on stochastic costs outperforms the deterministic approach by up to 15%, as it reveals 'hidden' downstream recovery potentials. This results in different slot allocations and in fewer passengers missing their connections.

INDEX TERMS Delay propagation, flight prioritization, schedule recovery, stochastic delay costs.

I. INTRODUCTION

At the tactical planning level, airlines are frequently required to prioritize between their flights due to short-term changes during the day of operations. These can be caused, for example, by capacity constraints at airports or in airspace [1]. In this context, the flight prioritization process aims at protecting the business utility of individual flights in the airline's network [2] by redistributing (assigned Air Traffic Flow Management (ATFM)) delays from aircraft with cost-intensive downstream constraints onto those which obtain high absorption or recovery capacities throughout their daily rotation. Cost-intensive downstream constraints may be disrupted passenger transfers at the destination of a delayed flight as well as crew duty time or airport curfew infringements. However, the identification of all constraints and potential recovery capacities as well as the estimation of the associated costs is not straightforward, especially when considering the low level of integration and automation in airline operations control [3]–[5]. In addition, actual flight and ground times are subject to a variety of uncertainties. For example, the uncertainty about a given primary delay propagating to a particular downstream constraint naturally increases with look-ahead time and the number of intermediate flights (air and ground segments). Due to the close links in the air traffic system, a delay obtained by one flight may spill onto several subsequent flights (reactionary delay) and have a lasting impact on the efficiency of scheduled operations.

The associate editor coordinating the review of this manuscript and approving it for publication was Nabil Benamar.

A. STATUS QUO ON DELAY PROPAGATION

Reactionary delay has been reported to be the largest contributor to departure delays in Europe [6], displaying an approximate ratio of 45% for many years. Reactionary delay is defined as the share of an arrival delay which cannot be absorbed by scheduled buffers or slack time during aircraft ground times, such that it propagates onto departure flights. Within airline networks, delay can be propagated within single aircraft rotations, i.e., rotational reactionary delay, or onto different aircraft due to passenger or crew transfers, i.e., non-rotational reactionary delay [7].

This work is licensed under a Creative Commons Attribution-NonCommercial-NoDerivatives 4.0 License. For more information, see https://creativecommons.org/licenses/by-nc-nd/4.0/

Delay propagation has been studied mainly retrospectively by building delay propagation trees with recorded timestamps from actual operations. A common metric to determine the impact of a schedule deviation in a given airline network is the "delay multiplier" [8]. This parameter describes the ratio of reactionary to primary delay and typically obtains higher values for larger deviations and for those that happen during morning operations.

Along with the delay multiplier as a measure of magnitude, further metrics have been introduced to characterise the impact of deviations on a flight-by-flight basis. These measures are severity, which defines the number of additionally affected flights, and depth, which determines the highest number of downstream legs impacted by propagated delay [9]. Initial models that studied delay propagation in airline networks considered a limited scope of resource dependencies and assumed static block times (i.e., scheduled flight time between off-block at origin and in-block at destination). These limitations were overcome with the help of Bayesian network models, that consider, for example, stochastic, non-independent and identically distributed block times when they analyse delay propagation trees at the strategic planning level (up to six months before operations). This enables the calculation of conditional probabilities for specific resources to contribute to the delay of a given flight and helps to eliminate them from future schedules [10], [11].

The magnitude and severity of a delay propagating through an airline network further depend on the business model and network strategy of the respective airline [12]. For instance, low-cost carriers tend to have very tight rotations with short turnaround times and few scheduled ground buffers, such that delays may propagate with a higher depth to several downstream flights of the same aircraft. At the same time, other rotations are less impacted, given that crew pairings typically follow the aircraft routing (i.e., few crew transfers) and no passenger transfers are sold within one ticket [9].

Conversely, full-service network carriers schedule longer ground times between their flights (at the airline hub airport), partially due to more extensive aircraft servicing activities [13], but also to increase the number of possible connections between flights [14]. In case of deviations from schedule or capacity constraints, such extended ground times may provide more absorptive capacities (i.e., buffers) along the aircraft rotation, which nevertheless incur high opportunity costs arising from reduced aircraft utilisation [15]. These opportunity costs drive airlines to continuously optimise their flight schedules, such that there is a variety of studies aiming at redistributing buffer capacities [16], [17] and synchronising aircraft, crew and passenger schedules to compensate for frequent delays and limit delay propagation [18]–[21].

Furthermore, robust fleet assignment strategies have been developed which aim at reducing the severity of a primary delay. This is accomplished, e.g., by assigning aircraft to fly so-called short cycles, which means that they directly return to the hub after flying to an out-station [22]. This limits the geographical scope in which a fleet is operating and helps to contain disruptions within a predefined area of the network [23]. However, it also triggers a phenomenon called back-propagation, that describes the effect when an airport is suffering from the reactionary delay that originated at the same airport earlier in the day [24]. Given that many hub airlines have implemented short cycles into their schedules in recent years, back-propagation is mainly experienced at major hub airports. Thereby, individual chain effects from and to particular airports appear to be volatile daily, considering frequently changing aircraft rotations and passenger demand [24], [25].

B. STATUS QUO ON AIRLINE SCHEDULE RECOVERY

In general, hub-and-spoke networks induce a higher level of complexity for tactical airline schedule recovery: First, economies of scope in a hub network result in very heterogeneous flight utilities, given that customers from many markets and with multiple flight legs may fly together on the same flight. This wide product scope often implies a wide range of fares and potentially higher compensation and reimbursement to be paid by the airline in case of schedule disruptions (see EU Regulation 261 [26]). Second, many crew and passenger transfer connections are likely to foster non-rotational delay propagation. Thereby, determining the impact of a specific delay on the entire network is particularly challenging if one considers that the monitoring and control process within an Airline Operations Control Center (AOCC) is still operated manually. This means that separate solutions are calculated for aircraft, crew and passenger recovery by applying general 'rules-of-thumb' with the help of database query systems. These department-specific solutions are collected centrally and it is up to the experience of the manager-on-duty to assemble a feasible recovery decision that satisfies the constraints of all involved departments and stakeholders [3]. Given a setting at major hub airports, where up to 100 aircraft of the same airline are turned around during so-called hub-banks within a time frame of about three hours, this can be a highly iterative and lengthy procedure and is unlikely to result in cost-minimal solutions. Consequently, many research projects aim at integration and partial automation of the decision-making process in an AOCC [27], [28].

Thus, some scholars see the highest potential to recover delays in changing critical aircraft and crew assignments, which may even include the cancellation of flight cycles to mitigate schedule disruptions [3], [4], [29]–[33]. Some studies further consider dynamic cost indexing, i.e., speeding up the flight cruise segment to reduce arrival delays [33] and some compare it to retiming the departure of other aircraft to ensure passenger transfers [34]–[38]. Other approaches have a local focus and consider recovery options mostly during the turnaround at a major airport, which includes the possibility to shorten or omit entire sub-processes, or assign extra resources to speed up standard operating procedures [5], [39]–[44].

The variety of approaches is also reflected by the incorporated objectives, which aim at minimising flight and/or passenger delays [42], [44]–[46], while others set out to optimise the associated cost of delay and recovery [5], [30], [32], [33], [35], [43], [47]. The latter objective includes the optimal assignment of recovery options to those flights with the highest priority (business utility), which is reflected by a progressive increase of costs at higher departure delays [7], [46].

European airline delay cost reference values have been modelled for different aircraft types, including, fuel, crew, maintenance, passenger 'hard' costs (e.g., care, rebooking, compensation) and 'soft' costs (e.g., market share attributable to punctuality) [7], [48]. However, they are not intended for prioritizing between particular flights, as they demonstrate monotonic, increasing delay cost functions. Underlying cost steps, largely driven by EU Regulation 261 [26], crew duty time regulations [49] and airport curfew costs [48], are smoothed by statistical fits and the effects of delay absorption through schedule buffers [7]. Conversely, flight-specific cost functions, which include cost steps for critical interdependencies between delays and downstream constraints, have so far only be been modelled schematically [2], [50], [51], e.g., for the validation of tactical flight prioritization mechanisms, such as the User-Driven Prioritisation Process (UDPP) [52]. Such schematic cost functions neglect detailed scheduling relationships as well as uncertainties related to the complexity and look-ahead time of downstream operations. This simplification might be attributed to data confidentiality reasons but also to the fact that forecasting delay impacts onto future operations requires a vast amount of historical data (categorised according to conditional probabilities) and a complex time-space model to consider the entire airline network for at least one day of operations [53]–[56].

C. FOCUS, CONTRIBUTION, AND STRUCTURE

From the status quo we derive two research gaps that are focused on in this article: 1) local schedule recovery models for the turnaround as well as recently proposed UDPP mechanisms for the tactical prioritization of flights, require airlines to have flight-specific delay cost models, such that downstream operations can be considered without having to model all processes explicitly; and 2) the delay cost estimation for a flight needs to consider conditional probabilities and increasing uncertainty associated with operational constraints further into the future.

For the prioritization of flights, we provide a flight-specific mathematical formulation for the cost of delay. To the best of our knowledge, this is the first time that a delay cost formulation is provided that considers all downstream constraints and recovery capacities within an aircraft rotation for an entire day of operations. This allows airlines to increase the efficiency of their local schedule recovery at major airports, such that constrained resources can be allocated to critical aircraft turnarounds and inevitable delays can be assigned to those flights that are least critical for the downstream network. All this can be achieved without having to model time-space relationship within the downstream network explicitly, which reduces the complexity of the studied process network.

The mathematical formulation is extended to describe the novel concept of stochastic delay cost functions. These functions provide a pro-active assessment of delay propagation and its related costs under uncertainty. Considering conditional probabilities and increasing uncertainty related to more distant operational constraints is deemed more realistic than a deterministic approach and this article studies whether the application of stochastic costs may render some otherwise needed recovery options unnecessary.

We structure this article as follows. Section II describes the methodology for building deterministic and stochastic delay cost functions. Section III describes how these cost functions can be incorporated into an airline schedule recovery model. Section IV demonstrates how deterministic and stochastic delay cost functions are derived within an airline case study network and defines scenarios that require their application in the context of tactical schedule recovery. Section V presents the results of the scenario analysis, from which Section VI draws conclusions and discusses potential future research.

II. MODELLING OF DELAY COST FUNCTIONS

Flight-specific delay cost functions are necessary to incorporate downstream network constraints and recovery capacities into the local optimisation context of schedule recovery, e.g., at an airline hub airport. This section details how these constraints and recovery capacities can be considered to respect succeeding flights in the aircraft routing, crew duty time regulations, passenger transfer connections or night curfews at subsequent airports.

A. DETERMINISTIC STEP COST FUNCTIONS

Let v_e^A be the arrival delay of a flight e from the set ARR of all arrival flights of an airline to its hub airport. The delay of this flight $e \in ARR$ may propagate into departure delay v_f^D of other flights f from the set of all departure flights DEP of that same airline.

The costs of departure delay $C_f^D(v_f^D)$ for a flight $f \in DEP$ can then be modelled as a function of v_f^D that includes flight delay costs $C_f^{\mathrm{DEP}}(v_f^D)$ for flight $f \in DEP$; flight delay costs $C_g^{\mathrm{ROF}}(v_f^D)$ for all other flights $g \in ROF$ operated by the same aircraft as part of its rotation on that day; flight delay costs $C_h^{\mathrm{NRF}}(v_f^D)$ for all flights $h \in NRF$ that are not part of the aircraft rotation but are connected to the delayed aircraft via passenger (PAX) transfer connections; costs of cancellation C_x^{CNX} of any downstream rotational flight $x \in DEP \cup ROF$ due to duty time, maintenance or curfew infringements; costs for passengers (or crew) missing their connections C_{fh}^{PAX} from departure flight f to any flight $h \in NRF$ – determined by $\kappa_{fh} \in \{0, 1\}$; and costs of passengers (or crew) missing their connections C_{gh}^{PAX} from any other rotational flight $g \in ROF$ to any non-rotational flight $h \in NRF$ – determined by $\kappa_{gh} \in \{0, 1\}$ (1). Fig. 1 exhibits the corresponding relationships

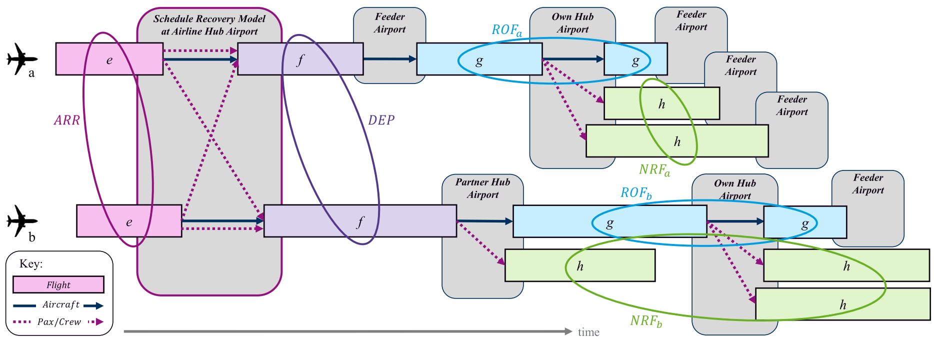

FIGURE 1. **Sets of flights considered within each aircraft rotation.**

within two example aircraft rotations.

$$\begin{aligned} C_f^D(v_f^D) = &\; C_f^{\mathrm{DEP}}(v_f^D) + \sum_{g \in \mathrm{ROF}} C_g^{\mathrm{ROF}}(v_f^D) \\ &+ \sum_{h \in NRF} \left(C_h^{\mathrm{NRF}}(v_f^D) \left(1 - \kappa_{fh}(v_f^D) - \kappa_{gh}(v_f^D)\right)\right) \\ &+ \sum_{x \in DEP \cup ROF} C_x^{\mathrm{CNX}}(v_f^D) \\ &+ \sum_{h \in \mathrm{NRF}} \left(C_{fh}^{\mathrm{PAX}}(att_h)\, N_{fh}^{\mathrm{PAX}}\, \kappa_{fh}(v_f^D)\right) \\ &+ \sum_{g \in \mathrm{ROF}} \sum_{h \in NRF} \left(C_{gh}^{\mathrm{PAX}}(att_h)\, N_{gh}^{\mathrm{PAX}}\, \kappa_{gh}(v_f^D)\right) \quad (1) \end{aligned}$$

Costs of flight delay consist of additional crew wage costs $C_f^{\mathrm{CRW},Aty}(v_f^D)$, additional maintenance costs $C_f^{\mathrm{MRO},Aty}(v_f^D)$ and costs of passenger dissatisfaction $C_f^{\mathrm{DIS},Aty}(v_f^D)$, which all depend on the aircraft type Aty and can be all modelled as (piece-wise) linear cost functions of the departure delay v_f^D (2). Thereby, the piece-wise linearisation of passenger dissatisfaction costs provides a good fit to the logit function of marginal soft costs [57], such that the resulting flight delay cost function is also piece-wise linear (see Fig. 2a). Modelling the delay costs of all rotational flights C_g^{ROF} and non-rotational flights C_h^{NRF} as a function of v_f^D provides the possibility to include scheduled buffers between flights, such that flights with higher buffers induce costs only at higher delays (see Fig. 2b and 2c). Note in Fig. 2c the dependency of flight delay costs on the respective aircraft type.

The costs of passengers missing their transfer connections C_{fh}^{PAX}, C_{gh}^{PAX} contain all monetary consequences for an airline that may arise once a group of transfer passengers N_{fh}^{PAX}, N_{gh}^{PAX} between flights f and g or h does not depart and/or arrive as scheduled (due to reasons for which the airline is liable). This includes basic administrative costs $C_{xh}^{\mathrm{BAS},Dist_{xh}}(att_h)$ and, according to EU Regulation 261 [26], costs of care $C_{xh}^{\mathrm{CAR},Dist_{xh},\lambda_1}(att_h)$, costs of compensation $C_{xh}^{\mathrm{COM},Dist_{xh},\lambda_2,\lambda_4}(att_h)$ (only if the airline is liable for the delay and the passenger is not reimbursed), costs of ticket rebooking $C_{xh}^{\mathrm{REB},Dist_{xh},\lambda_4}(att_h)$, costs of reimbursement $C_{xh}^{\mathrm{REI},Dist_{xh},\lambda_3,1-\lambda_4}(att_h)$ (only if passengers do not fly with an alternative flight) and costs of lodging $C_{xh}^{\mathrm{LOD}}(att_h)$ in case no alternative flight is available before the next day or passengers abandon the journey. Most of these costs depend on the combined trip distance $Dist_{xh}$ of flights $x \in DEP \cup ROF$ and $h \in NRF$ and the additional trip time att_h with alternative flights to h, which imply the arrival delay at the final destination and need to be deducted to respect historical claim ratios ($\lambda_1 - \lambda_4 \in (0, 1)$) [48], [57].

$$C_f^{\mathrm{DEP}}(v_f^D) = C_f^{\mathrm{CRW},Aty}(v_f^D) + C_f^{\mathrm{MRO},Aty}(v_f^D) + C_f^{\mathrm{DIS},Aty}(v_f^D) \quad (2)$$

$$C_g^{\mathrm{ROF}}(v_f^D) = C_g^{\mathrm{CRW},Aty}(v_f^D) + C_g^{\mathrm{MRO},Aty}(v_f^D) + C_g^{\mathrm{DIS},Aty}(v_f^D) \quad (3)$$

$$C_h^{\mathrm{NRF}}(v_f^D) = C_h^{\mathrm{CRW},Aty}(v_f^D) + C_h^{\mathrm{MRO},Aty}(v_f^D) + C_h^{\mathrm{DIS},Aty}(v_f^D) \quad (4)$$

$$\begin{aligned} C_{xh}^{\mathrm{PAX}}(att_h) = &\; C_{xh}^{\mathrm{BAS},Dist_{xh}}(att_h) + C_{xh}^{\mathrm{CAR},Dist_{xh},\lambda_1}(att_h) \\ &+ C_{xh}^{\mathrm{COM},Dist_{xh},\lambda_2,\lambda_4}(att_h) + C_{xh}^{\mathrm{REB},Dist_{xh},\lambda_4}(att_h) \\ &+ C_{xh}^{\mathrm{REI},Dist_{xh},\lambda_3,1-\lambda_4}(att_h) + C_{xh}^{\mathrm{LOD}}(att_h) \quad (5) \end{aligned}$$

Fig. 2d shows potential cost functions across all hauls, when 80% of passengers would accept meal vouchers ($\lambda_1 = 0.80$), 58% would apply for compensations ($\lambda_2 = 0.58$), 50% would claim reimbursements ($\lambda_3 = 0.50$), 80% would opt for being rebooked ($\lambda_4 = 0.80$), while 20% are assumed to abandon the trip and are ineligible for compensations [48].

As noted above, if a passenger transfer is rebooked, the binary variables $\kappa_{fh}(v_f^D)$ or $\kappa_{gh}(v_f^D)$ take a value of 1. The formulation of this variable as a function of the departure delay v_f^D allows the incorporation of the slack time until a transfer needs to be rebooked. Furthermore, it enables the consideration of an additional waiting time which may be predefined in the airline recovery policy, e.g., maximum 10 minutes delay per flight before downstream transfer passengers are rebooked (see Fig. 2e). Finally, Fig. 2f displays a flight-specific delay cost function with respect to the number of passengers per transfer.

In order to include this function within a Mixed-Integer Linear Programming (MILP) formulation, the total delay v_f^D obtained by a flight $f \in DEP$ is distributed across several delay levels L, such that the delay r_{fl} in each level $l \in L$

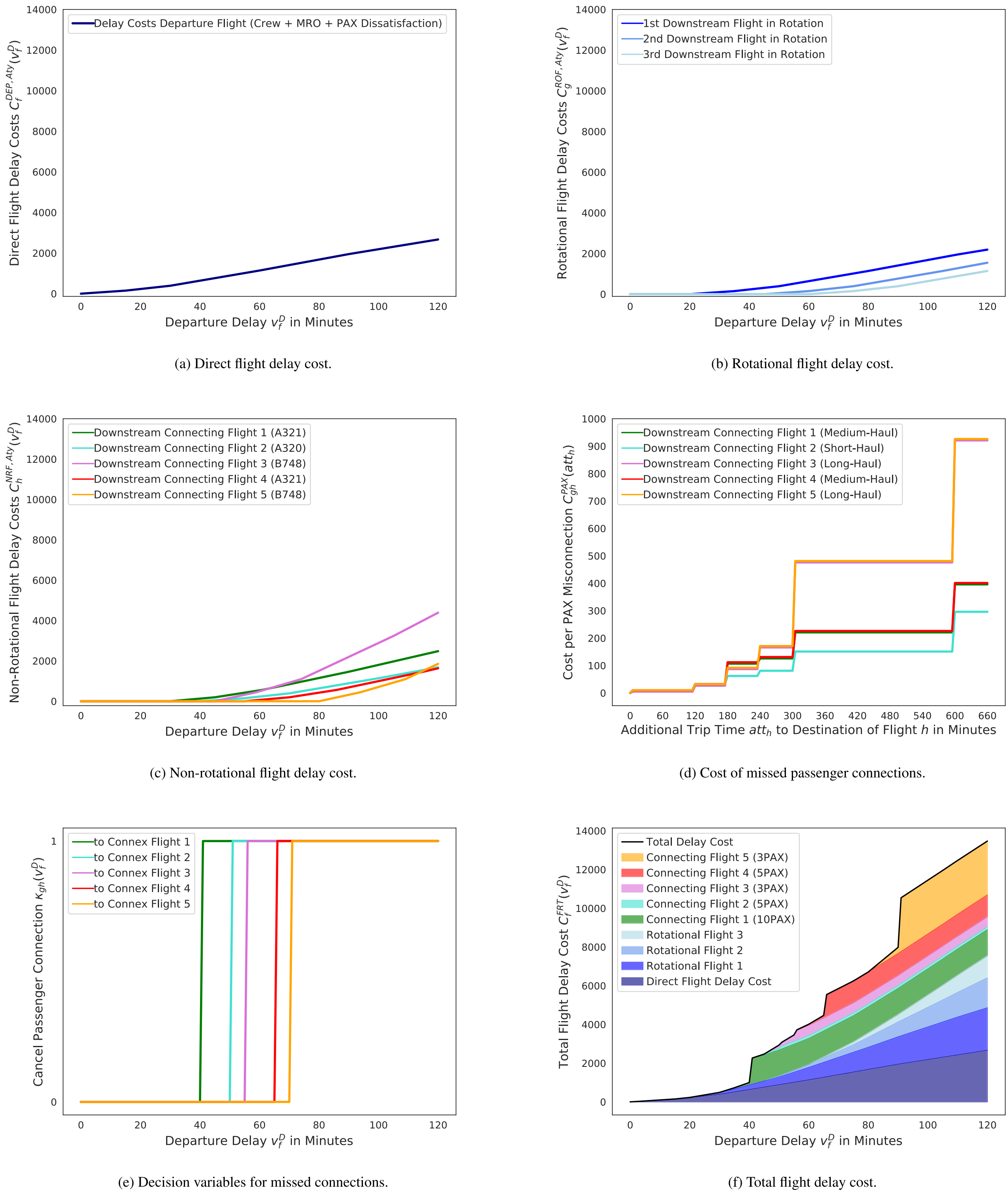

(a) Direct flight delay cost.

(b) Rotational flight delay cost.

(c) Non-rotational flight delay cost.

(d) Cost of missed passenger connections.

(e) Decision variables for missed connections.

(f) Total flight delay cost.

FIGURE 2. Components of a flight-specific delay cost function.

incurs constant marginal (linear) delay costs C_{fl}^{Dl} and has an upper bound UB_{fl} and a lower bound LB_{fl} (see Fig. 3). Once the buffer time before critical downstream constraints in an aircraft rotation is consumed, which is determined by $y_{fl} \in \{0, 1\}$; step costs C_{fl}^{Ds} are incurred in between two delay levels. Although this formulation would allow individual lengths for each delay level, a general version may foresee standardised delay levels of five minutes.

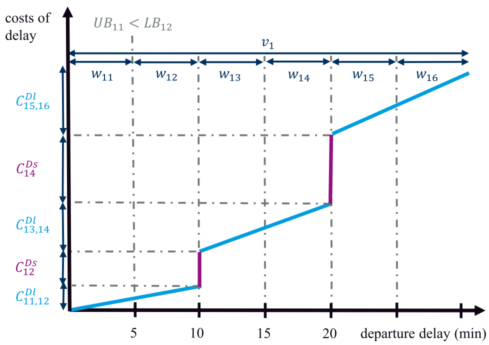

FIGURE 3. Mathematical representation of a step linear delay cost function in the MILP.

B. STOCHASTIC DELAY COST FUNCTIONS

The stochastic cost model builds on the flight-specific delay cost model and incorporates stochastic block and ground times for and between the upcoming flight legs in the respective aircraft rotation. These can be derived as conditional probabilities from historical operations data, such that they indicate how much of a given departure delay v_f^D of flight $f \in DEP$ at the hub is likely to propagate into an arrival delay v_f^A at the out-station, a departure delay v_g^D at the out-station and an arrival delay back at the hub v_g^A of a subsequent flight $g \in ROF$ in the aircraft rotation (see Fig. 4). The latter was described as back-propagation in Section I and may influence also further short-cycles afterwards, which are more difficult to incorporate because of frequently changing aircraft routings as further elaborated in Section IV. Learning such probabilities from historic data can reveal otherwise confidential airline data or delay influences which are difficult to predict and depend on a range of side factors, such as inherent block-time buffers, traffic, the potential of dynamic cost indexing or ground operations performance at an out-station [56].

In any case, the consideration of block and short-cycle time variance is deemed more accurate than the common assumption that departure delay propagates one-to-one into arrival delay and is thereafter only absorbed by ground buffers at the out-station [10]. Consequently, the stacked deterministic delay cost function in Fig. 2f needs to be unbundled once again, such that the individual cost factors can be accurately assigned to the operational milestones (e.g., in-block IB or off-block OB) in the downstream aircraft rotation. Thus, as detailed in Fig. 4, costs which arise from the duty of care according to EU Regulation 261 are directly attributable to departure delay at the hub. Costs for additional fuel burn and maintenance expenses may appear if the airline decides to mitigate part of the delay through dynamic cost indexing. All other costs are only incurred in case that a departure delay induces an arrival delay. Departure delay costs at the out-station arise from the same factors as at the hub, but only in case the arrival delay also propagates from the first to the second flight leg. Finally, the second stage of arrival delay costs depend on how much delay can be absorbed during the second block time and how much is still propagated back to the hub and further on.

Stochastic block-, ground or even entire short-cycle time distributions can be fitted from field data, whereby they are categorised depending on the amount of departure delay v_f^D obtained at the origin airport of flight f. Fig. 5a shows probability density functions for 10-minute categories of departure delay between 0 and 60 minutes with a block time standard deviation of 5 minutes. For each category, the deterministic cost function of the respective downstream milestone $C_f^A(v_f^D)$, e.g., arrival delay of flight f, is integrated with the conditional probability $p(v_f^A \mid v_f^D)$ of the departure delay propagating to that milestone. Subsequently, the cost integrals from all milestones need to be stacked to calculate the stochastic delay costs $SC_f^D(v_f^D)$ for this category of departure delay. The entire stochastic delay cost function exhibited in Fig. 5b may then be described by calculating the summed integral for all delay categories and then fitting all integral values with a piece-wise linear function (6) - (10).

$$
\begin{aligned}
SC_f^D(v_f^D) = {} & C_f^D(v_f^D) + \int \left(p(v_f^A \mid v_f^D) \cdot C_f^A(v_f^A)\, dv_f^A \right) \\
& + \sum_{g \in \mathrm{ROF}} \left(\int \left(p(v_g^D \mid v_f^D) \cdot C_g^D(v_g^D)\, dv_g^D \right) \right) \\
& + \sum_{g \in \mathrm{ROF}} \left(\int \left(p(v_g^A \mid v_f^D) \cdot C_g^A(v_g^A)\, dv_g^A \right) \right) \qquad (6)
\end{aligned}
$$

$$
C_f^D(v_f^D) = C_{ef}^{\mathrm{CAR},Dist_{ef},\lambda_1}(v_f^D) \qquad (7)
$$

$$
\begin{aligned}
C_f^A(v_f^A) = {} & C_f^{\mathrm{DIS},Aty}(v_f^A) + C_f^{\mathrm{CRW},Aty}(v_f^A) \\
& + C_f^{\mathrm{MRO},Aty}(v_f^A) + C_x^{\mathrm{CNX}}(v_f^A) \\
& + \sum_{h \in NRF} \left(C_{fh}^{\mathrm{PAX}}(att_h)\, N_{fh}^{\mathrm{PAX}}\, \kappa_{fh}(v_f^A) \right) \\
& + \sum_{h \in NRF} \left(C_h^{\mathrm{NRF}}(v_f^A)\, (1 - \kappa_{fh}(v_f^A)) \right) \qquad (8)
\end{aligned}
$$

$$
C_g^D(v_g^D) = C_{fg}^{\mathrm{CAR},Dist_{fg},\lambda_1}(v_g^D) \qquad (9)
$$

$$
\begin{aligned}
C_g^A(v_g^A) = {} & C_g^{\mathrm{DIS},Aty}(v_g^A) + C_g^{\mathrm{CRW},Aty}(v_g^A) \\
& + C_g^{\mathrm{MRO},Aty}(v_g^A) + C_g^{\mathrm{CNX}}(v_g^A) \\
& + \sum_{h \in \mathrm{NRF}} \left(C_{gh}^{\mathrm{PAX}}(att_h)\, N_{gh}^{\mathrm{PAX}}\, \kappa_{gh}(v_g^A) \right) \\
& + \sum_{h \in NRF} \left(C_h^{\mathrm{NRF}}(v_g^A)\, (1 - \kappa_{gh}(v_g^A)) \right) \qquad (10)
\end{aligned}
$$

Note that the generalised version depicted in Fig. 5 assumes normal-distributed block times with constant variance across all departure delay categories. This is independent of the true stochastic nature of a particular flight, where one may find best fits with, e.g., Beta- or Weibull-distributions [58]. In any case, smaller standard deviations result in stochastic delay cost functions that closely fit the shape of the deterministic cost curves, whereas large standard deviations smooth the curve along the x-axis

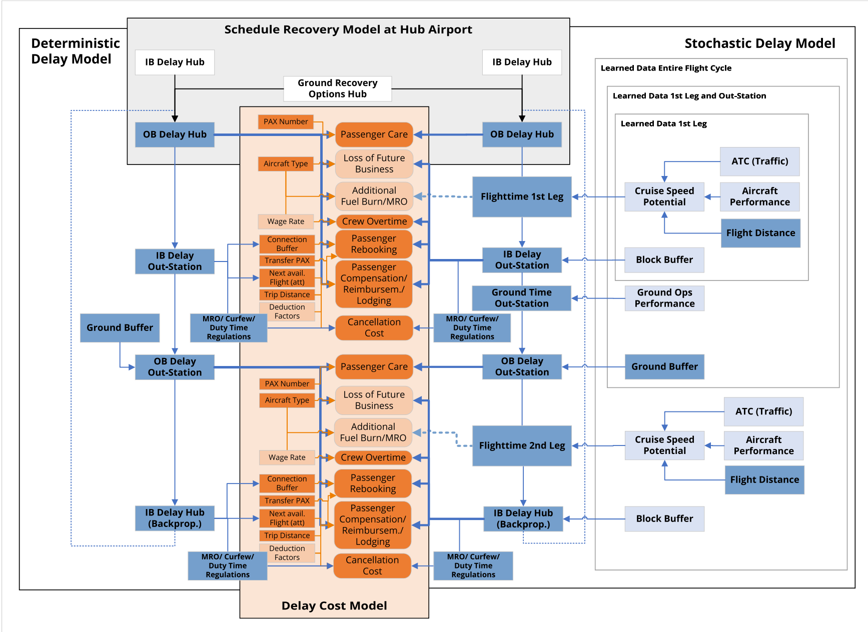

FIGURE 4. **Framework of stochastic delay costs. For an improved situational awareness during tactical schedule recovery, downstream uncertainties are considered while modelling delay propagating along an aircraft rotation. Dependencies from muted boxes are derived from field data.**

(see Figs. 5c and 5d). If the scheduled block time comprises buffer times, the stochastic cost curve is shifted towards the right on the x-axis, whereas actual block times that exceed the scheduled period cause a dislocation towards the left (see Figs. 5e and 5f). Depending on the block-time characteristics of a specific flight, multiple parameters can interfere with another and distort the stochastic function in the directions described.

III. IMPLEMENTATION INTO TACTICAL AIRLINE SCHEDULE RECOVERY

As described, delay cost functions may support tactical airline schedule recovery, such that ATFM slots or constrained resources for the turnaround can be assigned preferably to those aircraft from whose subsequent flights the airline is likely to incur higher costs of delay. Thus, deterministic and stochastic delay cost functions from the previous section are implemented into a scheduling model for tactical airline schedule recovery, described in full detail in [5].

A. AIRLINE SCHEDULE RECOVERY IN CONSTRAINTS

The schedule recovery model aims at assigning a limited set of ATFM slots and ground handling standard and reserve resources to a set of aircraft AC, such that tactical airline costs within a given airport capacity constraint are minimised.

All slots for arrival flights of an airline during a constraint are defined as set AS, while all slots for departure flights are defined as set DS. The assignment of an aircraft a from the set of all aircraft AC to an arrival slot $s \in AS$, is done with $z^A_{es} \in \{0, 1\}$; whereas a departure slot $s \in DS$ is assigned with $z^D_{fs} \in \{0, 1\}$; Each slot defines a calculated take-off time $CTOT_s$ and a required time of arrival RTA_s, which are calculated according to the Ration-by-Schedule (RBS) principle for each flight of the airline within the constraint considering all flights of other airlines [51]. In the baseline instance, each flight is fixed to its assigned slot respecting a First-Planned First-Served (FPFS)-sequence. In case this is infeasible because there is not enough time for the turnaround between assigned arrival and departure slots, alternative slots are available after the last flight of the airline in the constraint. For the scenarios introduced in Section IV-D, the fixed assignment can be lifted.

The turnaround of each aircraft $a \in AC$ is defined by scheduled start and finishing times $SIBT_e$ and $SOBT_f$, which are adopted from the schedule. It consists of a network of sub-processes P, in which each sub-process $i \in P$ is characterised by a related aircraft ($RA_i = a$) and a related flight ($RF_i = e, f$), has a variable starting time s_i and a duration D_i that corresponds to the median of a statistically-fitted time distribution [45]. Links between turnaround sub-processes are determined in the precedence matrix $PM_{ij} \subseteq P \times P$.

Following the general Resource-Constrained Project Scheduling Problem (RCPSP), each aircraft a needs to be assigned to an airport stand p from the set ST with $\chi_{ap} \in \{0, 1\}$, whereby we differentiate between contact stands CS and remote stands RS, that are all equipped with the necessary personnel and resources for a standard turnaround. Thus, the in-block process $i \in IB \subset P$, as the first process of each turnaround, can only be scheduled after the $SIBT_e$ and if a stand is available which fulfils all operational requirements for aircraft and flights. It further depends on the estimated landing time $eldt_e$ of the assigned slot and the average taxi-in duration $\overline{EXIT}$.

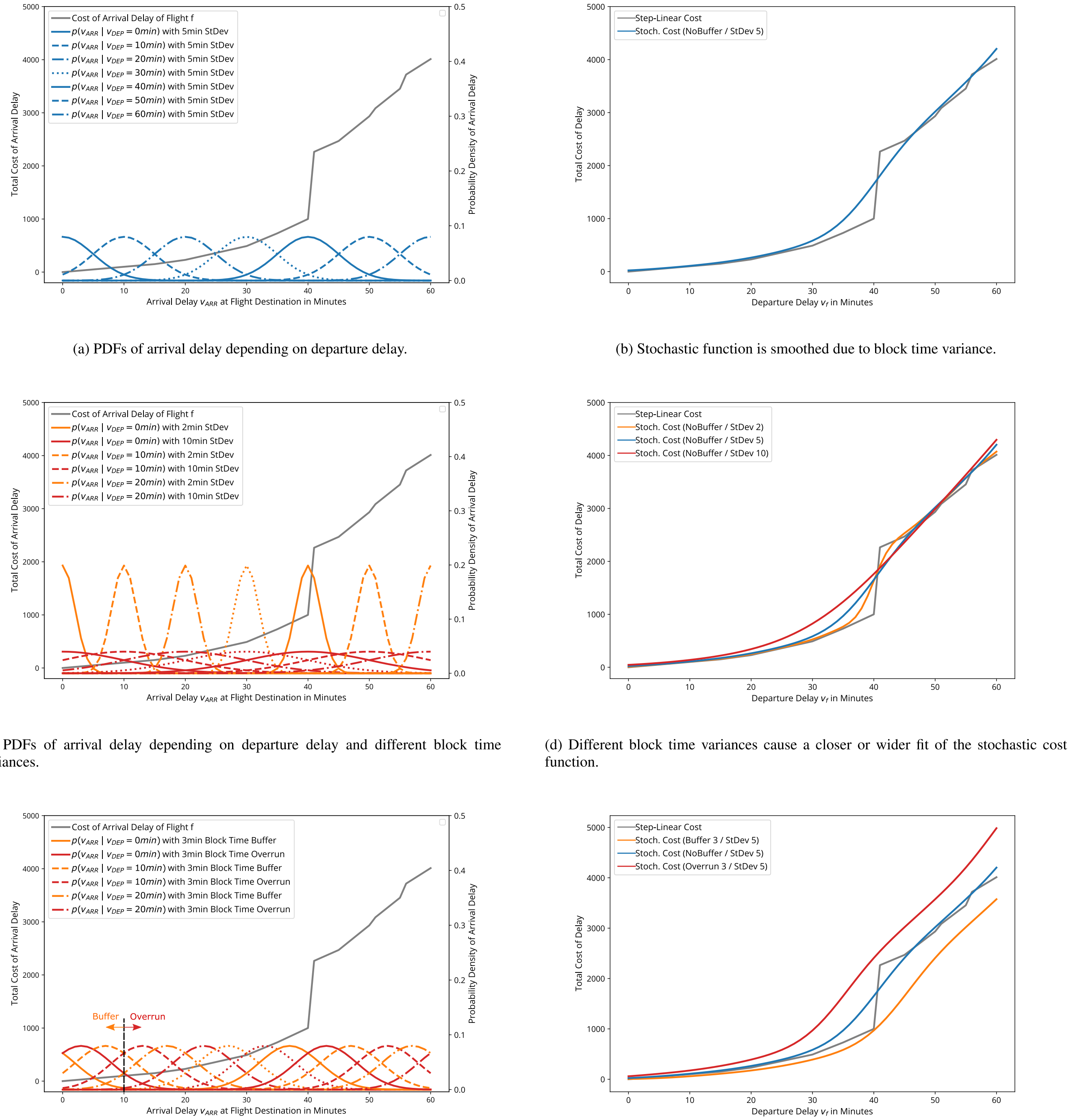

(a) PDFs of arrival delay depending on departure delay.

(b) Stochastic function is smoothed due to block time variance.

(c) PDFs of arrival delay depending on departure delay and different block time variances.

(d) Different block time variances cause a closer or wider fit of the stochastic cost function.

(e) PDFs of arrival delay depending on departure delay and different lengths of scheduled block time.

(f) Block time buffers/ overruns cause a dislocation of the stochastic function along the x-axis.

FIGURE 5. **Impact of block time variance and schedule parameters on delay cost function.**

Downstream sub-processes can only start once all preceding processes are estimated to be completed. Thereby, turnaround reserve resources enable schedule recovery options, such as a quick turnaround ($\omega_i \in \{0, 1\}$), which reduces the duration of specific turnaround sub-processes, e.g., cabin cleaning $i \in CL \subset P$. These reserve resources are limited by QTA and incur recovery costs C_i^{QTA} by each application. Another recovery option is stand reallocation which considers that aircraft that are positioned at a remote stands $p \in RS$ have reduced durations for de-/boarding processes $i \in DE, BO \subset P$, given that passengers can use front and rear doors [59]. It further considers that the stand allocation of arrival and departure aircraft at an airport directly influences the needed transfer time NTT_{pq} for connecting passengers. By applying these options, airlines can influence the total duration along the critical path of a turnaround but also time dependencies between aircraft along transfer processes $i \in PA \subset P$. If a transfer would require a departure flight to delay its off-block, the airline can either rebook the transfer ($\kappa_i \in \{0, 1\}$) or accept the delay. The prior decision would incur misconnection costs C_i^{PAX}, similar as described for downstream transfers in (5). In case the transfer involved a crew, it can only be cancelled if a standby crew is available. Delaying the departure of a flight incurs delay costs as described in Section II.

The estimated delay is split across equally sized delay levels $l \in L$ in which the delay r_{fl} has constant linear costs C_{fl}^{Dl}. In case of deterministic cost functions, step costs C_{fl}^{Ds} are incurred once the scheduled buffer or slack time before a critical downstream event is consumed (determined by $y_{fs} \in \{0, 1\}$). The resulting estimated off-block time $eobt_f$ is added with an average taxi-out duration $\overline{EXOT}$ to calculate the estimated take-off time $etot_f$, which needs to comply with the $CTOT_s$ of the assigned departure slot s.

B. MATHEMATICAL FORMULATION

SETS

AC	set of all aircraft
ARR	set of all arrival flights to airline hub airport
DEP	set of all departure flights from airline hub airport
P	set of all turnaround processes
$IB \subset P$	set of aircraft in-block processes
$DE \subset P$	set of deboarding processes
$CL \subset P$	set of cleaning processes
$BO \subset P$	set of boarding processes
$OB \subset P$	set of aircraft finalization processes
$PA \subset P$	set of passenger transfer processes
L	set of delay levels
ST	set of available stands at airport
$RS \subset ST$	set of available remote stands on airport apron
AS	set of all initial arrival slots assigned to the airline
DS	set of all initial departure slots assigned to the airline
$A0$	start and end node of routings

PARAMETERS

C_i^{QTA}	cost for reducing duration of process i by quick-turnaround
C_i^{PAX}	cost of cancelling a local passenger transfer $i \in PA$
C_{fl}^{Dl}	linear delay cost of flight $f \in DEP$ in delay level $l \in L$
C_{fl}^{Ds}	step cost of flight $f \in DEP$ after delay level $l \in L$
QTA	number of available quick-turnaround units
$SIBT_e$	scheduled in-block time for flight $e \in ARR$
$SOBT_f$	scheduled off-block time for flight $f \in DEP$
LB_{fl}	lower bound of delay level $l \in L$ for flight $f \in DEP$
UB_{fl}	upper bound of delay level $l \in L$ for flight $f \in DEP$
D_i	duration of turnaround sub-process $i \in P$
NTT_{pq}	transfer time between stands $p \in ST$ and $q \in ST$
TT	transition time between two stand assignments
α	time reduction factor achieved by quick-de/boarding
β	time reduction factor achieved by quick-turnaround
$\overline{EXIT}$	average taxi-in duration at hub airport
$\overline{EXOT}$	average taxi-out duration at hub airport
$CTOT_s$	calculated take-off time related to slot $s \in AS \cup DS$
RTA_s	required time of arrival related to slot $s \in AS \cup DS$
RA_i	related aircraft of turnaround sub-process $i \in P$
RF_i	related flight of turnaround sub-process $i \in P$
M	parameter-specific big M

VARIABLES

s_i	starting time of turnaround sub-process $i \in P$
v_f^D	total departure delay of departure flight $f \in DEP$
r_{fl}	delay of flight $f \in DEP$ in delay level $l \in L$
$y_{fl} \in (0; 1)$	equal to 1 if delay of flight $f \in DEP$ exceeds level $l \in L$
$eldt_e$	estimated landing time for arrival flight $e \in ARR$
$eobt_f$	estimated off-block time for departure flight $f \in DEP$
$etot_f$	estimated take-off time for departure flight $f \in DEP$
$\chi_{ap} \in (0; 1)$	equal to 1 if aircraft a is assigned to stand $p \in ST$
$\psi_{abpq} \in (0; 1)$	equal to 1 if aircraft a and b are assigned to stands p and q
$\omega_a \in (0; 1)$	equal to 1 if quick-turnaround is assigned to aircraft a
$\kappa_i \in (0; 1)$	equal to 1 if passenger transfer $i \in PA$ is cancelled

$z^A_{es} \in (0; 1)$	equal to 1 if flight $e \in ARR$ is assigned to arrival slot $s \in AS$
$z^D_{fs} \in (0; 1)$	equal to 1 if flight $f \in DEP$ is assigned to departure slot $s \in DS$
$xQ_{ab} \in (0; 1)$	sequencing variable for quick-turnaround procedures
$xS_{abp} \in (0; 1)$	sequencing variable for aircraft $a, b \in AC$ at stand $p \in ST$

$$\min \sum_{f \in DEP} \sum_{l \in L} \left(C^{Dl}_{fl}\, r_{fl} + C^{Ds}_{fl}\, y_{fl} \right) + + \sum_{i \in P} \left(C^{\text{QTA}}_i\, \omega_i + C^{\text{PAX}}_i\, \kappa_i \right) \tag{11}$$

s.t.

$$s_i \geq \text{SIBT}_e \quad \forall i \in IB \mid RF_i = e \tag{12}$$

$$s_i \geq \text{eldt}_e + \overline{\text{EXIT}} \quad \forall i \in IB \mid RF_i = e \tag{13}$$

$$\text{eldt}_e \geq \text{RTA}_s - M(1 - z^A_{es}) \;\; \forall e \in ARR; \forall s \in AS \tag{14}$$

$$\text{eldt}_e \leq \text{RTA}_s + M(1 - z^A_{es}) \;\; \forall e \in ARR; \forall s \in AS \tag{15}$$

$$\sum_{s \in AS} z^A_{es} = 1 \quad \forall e \in ARR \tag{16}$$

$$\sum_{e \in ARR} z^A_{es} \leq 1 \quad \forall s \in AS \tag{17}$$

$$s_i \leq \text{SOBT}_f + v^D_f = \text{eobt}_f \quad \forall i \in OB \mid RF_i = f \tag{18}$$

$$v^D_f = \sum_{l \in L} r_{fl} \quad \forall f \in DEP \tag{19}$$

$$r_{fl} \geq \left(UB_{fl} - LB_{fl} \right) y_{fl} \quad \forall f \in DEP; \forall l \in L \tag{20}$$

$$r_{fl} \leq \left(UB_{fl} - LB_{fl} \right) y_{f(l-1)} \quad \forall f \in DEP; \forall l \in L \tag{21}$$

$$\text{eobt}_f + \overline{\text{EXOT}} = \text{etot}_f \quad \forall f \in DEP \tag{22}$$

$$\text{etot}_f \geq \text{CTOT}_s - M(1 - z^D_{fs}) \quad \forall f \in DEP; \forall s \in DS \tag{23}$$

$$\text{etot}_f \leq \text{CTOT}_s + M(1 - z^D_{fs}) \quad \forall f \in DEP; \forall s \in DS \tag{24}$$

$$\sum_{s \in DS} z^D_{fs} = 1 \quad \forall f \in DEP \tag{25}$$

$$\sum_{f \in DEP} z^D_{fs} \leq 1 \quad \forall s \in DS \tag{26}$$

$$s_j \geq s_i + D_i \;\; \forall i \in IB, \;\; \forall j \in P \mid PM_{i,j} = 1 \tag{27}$$

$$s_j \geq s_i + D_i(1 - \chi_{ap}) + \alpha D_i \chi_{ap} \quad \forall i \in DE \cup BO, \forall j \in P \mid PM_{i,j} = 1; RA_i = a; \forall p \in RS \tag{28}$$

$$s_j \geq s_i + \text{NTT}_{pq} \psi_{abpq} - M \kappa_i \quad \forall i \in PA, \forall j \in P \mid PM_{i,j} = 1, RA_i = a, RA_j = b, \forall p, q \in ST \tag{29}$$

$$\chi_{ap} + \chi_{bq} \leq 1 + \psi_{abpq} \;\; \forall a, b \in AC; \forall p, q \in ST \tag{30}$$

$$\chi_{ap} \geq \psi_{abpq} \quad \forall a, b \in AC; \quad \forall p, q \in ST \tag{31}$$

$$\chi_{bq} \geq \psi_{abpq} \quad \forall a, b \in AC; \quad \forall pq \in ST \tag{32}$$

$$\sum_{p \in ST} \chi_{ap} = 1 \quad \forall a \in AC \tag{33}$$

$$\sum_{a \in AC \cup A0} xS_{abp} = \chi_{ap} \quad \forall b \in AC; \forall p \in ST \tag{34}$$

$$\sum_{b \in AC \cup A0} xS_{abp} = \chi_{ap} \quad \forall a \in AC; \forall p \in ST \tag{35}$$

$$s_j \geq s_i + TT - M(1 - xS_{abp}) \quad \forall a \in AC; \forall b \in AC \cup A0; \forall p \in ST; \forall i \in OB \mid RA_i = a; \forall j \in IB \mid RA_j = b \tag{36}$$

$$s_j \geq s_i + D_i(1 - \omega_i) + \beta D_i \omega_i \quad \forall i \in CL, \forall j \in P \mid PM_{i,j} = 1 \tag{37}$$

$$\sum_{b \in AC \cup A0} xQ_{ab} \leq \text{QTA} \quad \forall a \in A0 \tag{38}$$

$$\sum_{a \in AC \cup A0} xQ_{ab} = \omega_b \quad \forall b \in AC \tag{39}$$

$$\sum_{b \in AC \cup A0} xQ_{ab} = \omega_a \quad \forall a \in AC \tag{40}$$

$$s_j \geq s_i + TT - M(1 - xQ_{ab}) \quad \forall a \in AC; \forall b \in AC \cup A0; \forall i \in OB \mid RA_i = a \; \forall j \in IB \mid RA_j = b \tag{41}$$

The objective function (11) minimises total costs of delay and schedule recovery. This includes linear costs across all delay levels, step costs once a critical delay threshold is overrun (not in the stochastic model) and costs related to schedule recovery during the turnaround or the cancellation of transfer connections. Each turnaround can only start after the scheduled in-block time (12) and after the landing and taxi-in of the arrival flight (13), whereby the estimated landing time must align with required time of arrival of the assigned arrival slot (14)-(15). All arrival flights that are part of an airport constraint need to be assigned to exactly one arrival slot (16), while each slot can be used by maximum one flight (17). According to the assigned departure slot, departure delay is distributed across predefined delay levels (18)-(19) and is translated into an estimated take-off time (22). Each delay level in the deterministic cost model is bounded such that delay can only occupy upper levels by taking into account the related step costs before them (20)-(21). Departure slot constraints (23)-(26) are similar to arrival slot constraints (14)-(17).

Standard scheduling constraints (27) ensure that all turnaround sub-processes following the in-block process can only start once it has been finished. Similar scheduling constraints are defined for processes starting after deboarding and boarding (28), whereby the duration of both processes

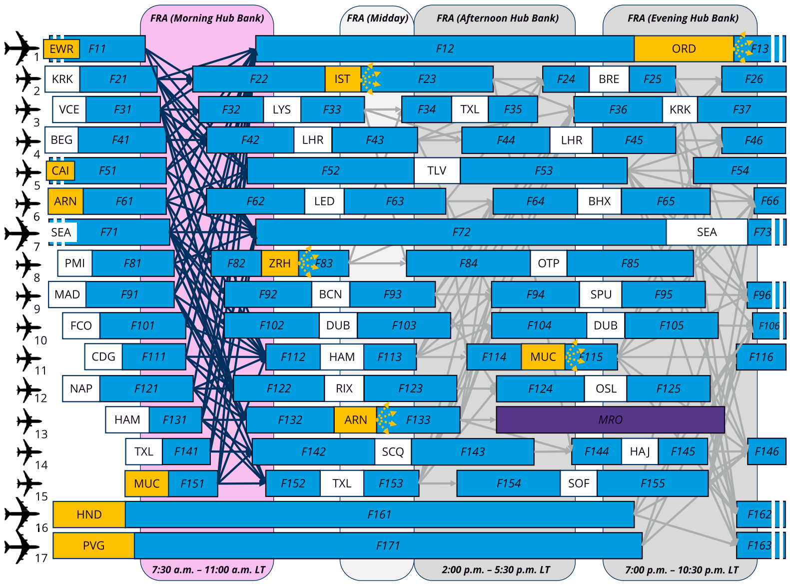

FIGURE 6. **Flight-specific delay cost functions are defined with respect to the constraints within an airline case study network, which includes one day of rotations for 17 aircraft between three major hub banks in Frankfurt (morning, afternoon, evening) as well as passenger and crew transfer connections between all flights. Spoke airports which are hub airports of partner airlines and allow further passenger transfer connections are marked in orange.**

can be reduced by a factor α when an aircraft is positioned at a remote stand $p \in RS$. Constraints (29) consider needed transfer times for connecting passengers and crews between the stands of their arrival and departure flights, which directly influences their stand allocation. Note that for the application of standard solvers, constraints (30)-(32) turn the quadratic relationship between both stand allocation variables into a linear formulation. Further note that transfer time dependencies are omitted for all transfer connections which are cancelled. Following the RCPSP, constraints (33) make sure that each aircraft is allocated to exactly one stand, whereby the Miller–Tucker–Zemlin (MTZ) formulation [60] in constraints (34)-(36) defines the sequence among aircraft which use equal stands and a dummy node $A0$, which marks the start and end of each sequence.

The standard RCPSP formulation is extended by the possibility to assign recovery resources to some turnaround sub-processes (e.g., cabin cleaning) which then reduce the respective durations by factor β (37). Considering that turnaround recovery resources are limited (38), another MTZ-formulation in constraints (39)-(41) builds a sequence that ensures that only so many turnarounds can be prioritized in parallel as recovery resources are available.

IV. APPLICATION

The schedule recovery model with deterministic and stochastic delay cost functions is applied to an airline case study network that is impacted by an airport capacity constraint (e.g., weather events [61]). This section presents the case study setting, exhibits the derived delay cost functions and introduces the disruption scenarios in which the airport operates with reduced runway capacity.

A. CASE STUDY SETTING

The airline case study network comprises 17 aircraft (four wide-body aircraft and 13 narrow-body aircraft), which are scheduled to operate 84 flights from and to the central hub at Frankfurt airport (FRA). All 17 aircraft rotations have been adopted from a publicly available Lufthansa schedule as planned for a busy Friday during the summer season 2019. This ensures that flight assignments adhere to aircraft characteristics and allows to incorporate realistic schedule buffers as optimised at the strategic planning level. Rotations are selected such that they include strategic destinations like hub airports of the Lufthansa Group and Star Alliance members [62]. One aircraft has a scheduled maintenance (MRO) event at FRA in the afternoon. Ten long-haul intercontinental flights are operated by long-haul aircraft (e.g., Boeing B748 and Airbus A388), whereas the remaining 74 flights are assigned to Airbus A320, A20N, A321 and A21N aircraft. The majority of aircraft meet during three hub banks throughout the day, from which the morning hub bank from 7:30 a.m. to 11:00 a.m. local time (highlighted in pink in Fig. 6) will represent the core of the case study. Consequently, parallel turnaround operations of 15 aircraft will be studied, which includes 151 passenger transfer connections and two crew transfers between their respective arrival and departure flights. All 15 turnarounds need to be operated at ten dedicated airport stands, of which eight are located at the terminal and two on the apron (see Fig. 7).

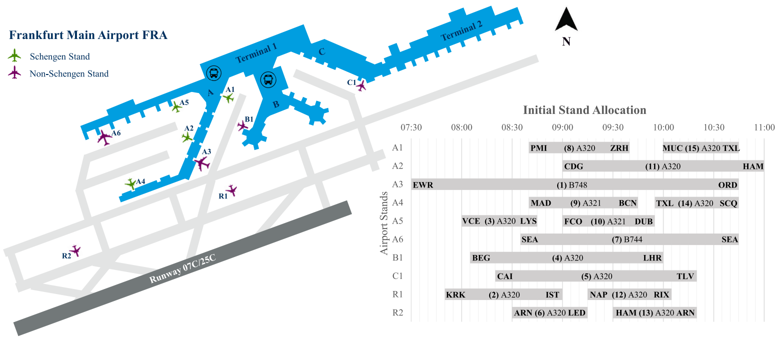

FIGURE 7. The analysis focuses on potential disruptions to aircraft ground times during the morning hub bank.

Among the stands at the terminal, four have special customs areas to operate Non-Schengen flights. Furthermore, each stand is assigned with the necessary ground handling resources and personnel to operate a standard turnaround, while one extra unit of servicing agents is freely available to perform quick-turnaround procedures. Furthermore, one dedicated bus allows the operation of ramp direct services on critical passenger connections, while one standby crew can step into duty in case of disrupted crew pairings.

Another 155 passenger transfers and six crew transfers are scheduled among downstream flights which will visit Frankfurt airport later during the day. Furthermore, 67 passenger itineraries include a transfer at the hub airport of a partner airline (marked in orange in Fig. 6).

B. DELAY COST PARAMETERS

As explained in (1)-(5) in Section II, flight delay costs of any flight $f \in DEP$ include additional crew wage costs for overtime in case the flight duty is scheduled to end after the departure flight from the hub, as well as additional maintenance costs and costs of passenger dissatisfaction. All depend on the respective aircraft type as described by [48], such that, e.g., one hour of overtime for an A320 flight crew (captain and first officer) and cabin crew (purser and three flight attendants) costs the airline 516 EUR, which splits into 8.6 EUR per minute of delay [63]. Additional maintenance costs are only minor and incur 0.5 EUR per delay minute, whereas passenger dissatisfaction costs are best modelled with logit functions [7], such that different gradients per delay level $l \in L$ are assumed for the first 15 minutes ($C_{f1}^{\mathrm{DIS},A320} =$ 1 EUR), delays between 16 and 30 minutes ($C_{f2}^{\mathrm{DIS},A320} =$ 6 EUR), between 31 and 60 minutes ($C_{f3}^{\mathrm{DIS},A320} = 16$ EUR), between 61 and 90 minutes ($C_{f4}^{\mathrm{DIS},A320} = 18$ EUR) and for delays above 90 minutes ($C_{f5}^{\mathrm{DIS},A320} = 15$ EUR).

Costs of passenger misconnections at downstream airports C_{fh}^{PAX}, C_{gh}^{PAX} are estimated with their respective transfer slack time as described in Section II. If a delay consumes the duty time buffer of a crew pairing or a crew misses its transfer to another flight, the costs of using a standby crew are 1,000 EUR. Flight cancellation costs due to maintenance constraints or night curfews include costs for dissatisfaction, rebooking, reimbursement and compensation for all passengers booked on the entire flight cycle (both legs), which corresponds to roughly 25,000 EUR per flight leg ($C_x^{\mathrm{CNX}} = 50{,}000$ EUR) as estimated by [4], [48].

Given that all mentioned cost-drivers on downstream flights are calculated as a function of the departure delay of departure flight $f \in DEP$ from the hub, buffer times between all flights before the actual event are accumulated and added to the planned crew transfer, passenger connection or curfew buffers (see Fig. 8). Thus, cost-drivers related to flights that are planned during the afternoon and evening hours may appear later on the delay cost function than events with similar slack or planned buffer times which are related to morning flights.

Note that some aircraft rotations do not contain any maintenance, curfew or crew transfer constraints, while the assigned crew pairings may have large duty time buffers, such that flight cancellation costs may be neglected entirely. Nevertheless, passenger transfer constraints and the related cost steps need to be considered in every delay cost function, given that each daily rotation includes at least one flight back to the hub airport, where passengers can transfer to other destinations. Thus, with an increasing number of downstream flight cycles, more cost steps may be part of the delay cost function, while also the slope increases due to more rotational flights being impacted by the delay (see continuous stars in Fig. 8). Further cost steps appear on rotations which include flight cycles to hub airports of partner airlines, given that passengers may have transfer connections to code-sharing flights.

C. ESTIMATION OF DOWNSTREAM UNCERTAINTY

For the consideration of uncertainty in downstream operations, actual flight data are retrieved for all departure flight rotations of the morning hub bank as operated during the summer season 2019 (217 days). As documented exemplary for the data set of aircraft 4 in Fig. 9, all data are filtered, such that only rotations are included that were operated by the same aircraft type as the first flight cycle on the case study day. Furthermore, rotations are excluded which had longer or shorter scheduled block or ground times during the first flight cycle. Subsequently, the remaining data

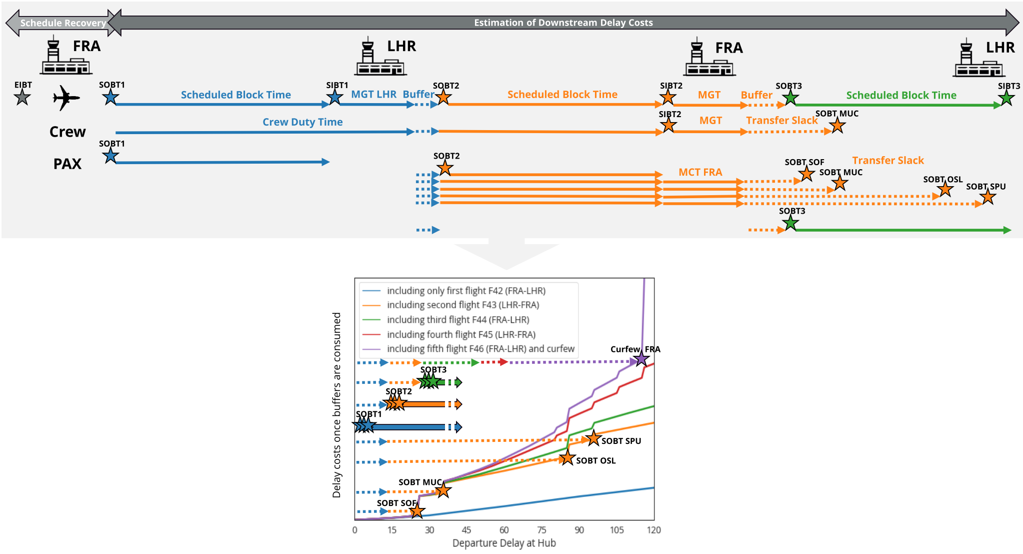

FIGURE 8. Cost-driving events (PAX rebookings, MRO events, crew changes, airport curfews) in downstream operations of each aircraft impact the airline once buffer and slack times (marked in dashed arrows) are consumed by a given primary delay.

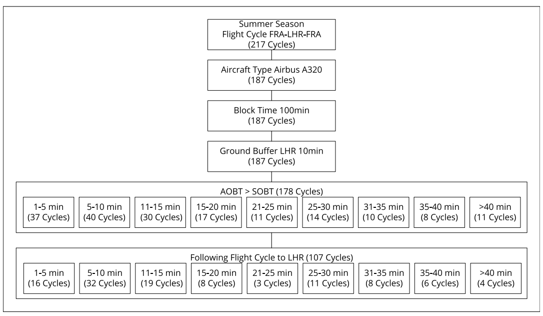

FIGURE 9. Data filtering process.

sets are categorised according to the amount of departure delay they obtained on their first flight out of the morning hub bank. Based on this selection, the probability density of the actual block time deviations from the scheduled times is calculated for each 5 minute category as shown in Fig. 10. The resulting distributions are integrated with the deterministic cost functions from the previous subsection to obtain a stochastic cost estimation at discrete grid points every 5 minutes. These grid points are connected with a piece-wise linear stochastic delay cost function as exhibited in Fig. 10i.

Considering that there have been only a few flight cycles with high departure delays, the probability density of the penultimate category is also used for all 5 minute categories above 40 minutes of delay. Here, the time horizon of the underlying data set needs to be extended to get a more comprehensive database per category. This is especially true when one considers that higher delays are typically associated with larger variances as will be further discussed in Section VI. The same is valid for longer look-ahead times, whereby the uncertainty estimation of milestones that are further down in the respective aircraft rotation is based on even smaller samples per delay category. As exhibited in Fig. 9, not even half of all seasonal rotations include the same set of flight cycles, both flying to LHR and back. Note here that on other rotations not even 5% of all seasonal rotations are equal to the ones observed on the day of the case study. To still consider uncertainties comprised within the third, fourth or even fifth downstream block time segments, the same categorical probability densities are applied to these flights as for the first flight cycle. In any case, this may easily be updated in future research once a larger database would be available.

Figs. 11 and 12 exhibit the resulting deterministic and stochastic delay cost functions for all departure flights of the morning hub bank. Note in Fig. 12 that several cost functions start increasing up to ten delay minutes after their deterministic counterparts, next to cost steps being smoothed due to block time variances. Furthermore, cumulative costs in higher delay levels, e.g., 120 minutes, are significantly lower due to block time buffers and cruise speed potential. The comparison with a reference cost function of an A320 [7] validates that all cost functions are in the right order of magnitude, given that the reference cost function shows similarity to a regression curve of the flight-specific cost functions. In any case, the heterogeneity of these flight-specific cost functions underlines their advantageous properties for tactical flight prioritization, which would be hard to accomplish for aircraft of the same type based on reference cost functions.

D. AIRPORT CONSTRAINT SCENARIOS

The nominal runway capacity at Frankfurt airport is defined with $AQ = 27$ movements per period of $PE = 15$ minutes.

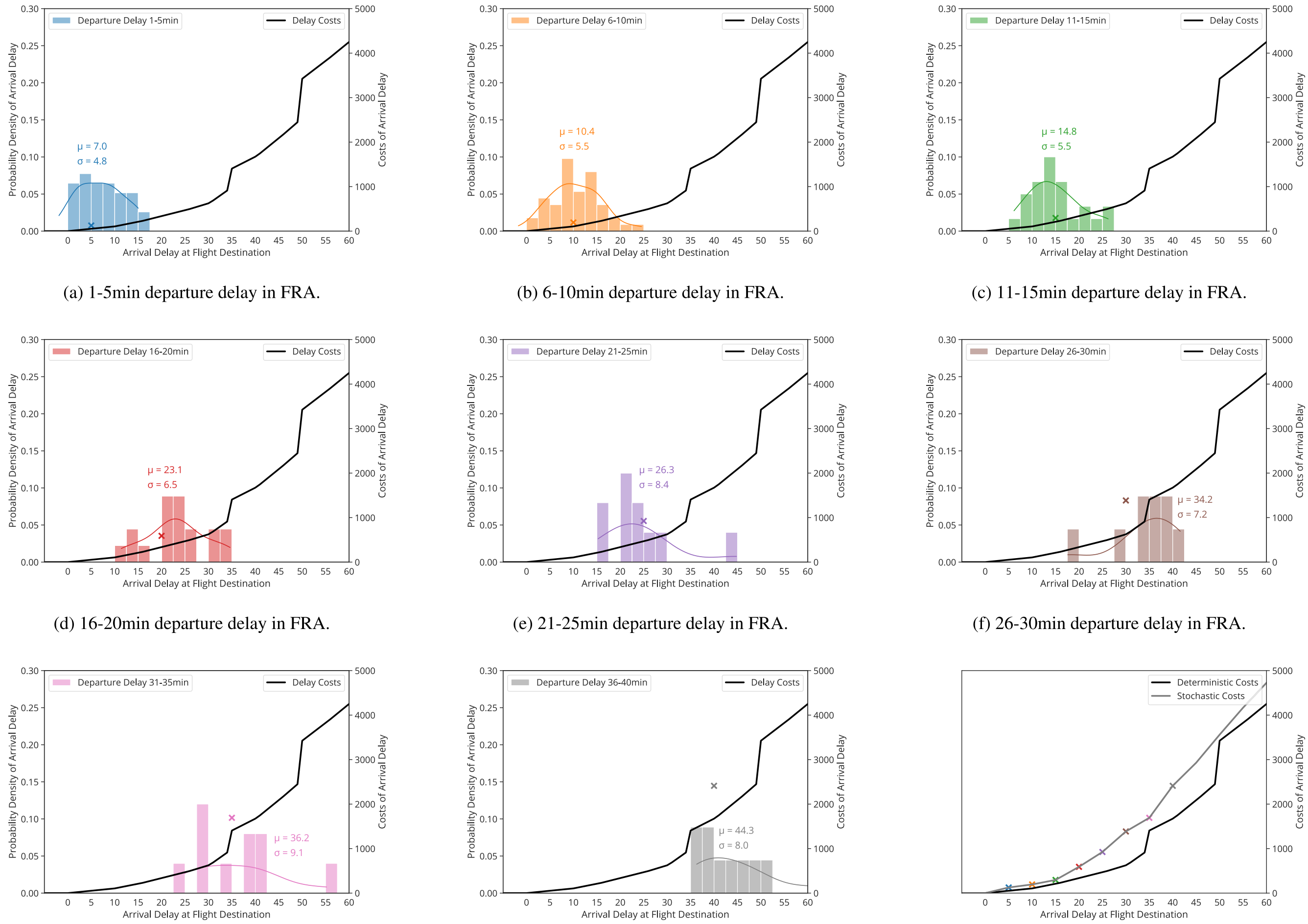

(a) 1-5min departure delay in FRA. (b) 6-10min departure delay in FRA. (c) 11-15min departure delay in FRA.

(d) 16-20min departure delay in FRA. (e) 21-25min departure delay in FRA. (f) 26-30min departure delay in FRA.

(g) 31-35min departure delay in FRA. (h) 36-40min departure delay in FRA. (i) Stochastic cost function.

FIGURE 10. The stochastic cost function is the piece-wise linearised result of an integration among a deterministic delay cost function and categorised block time deviations as observed on the flight cycle to London (LHR) during the summer season 2019.

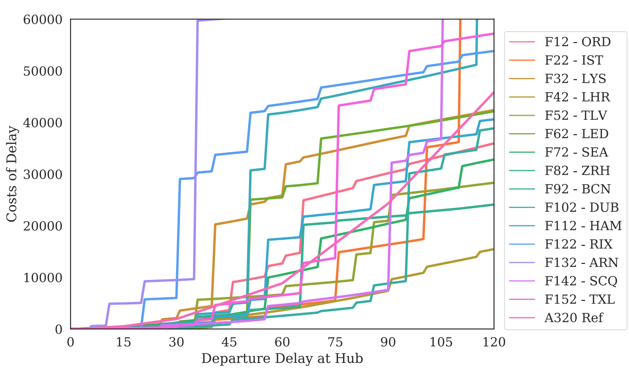

FIGURE 11. Deterministic delay cost function of all aircraft.

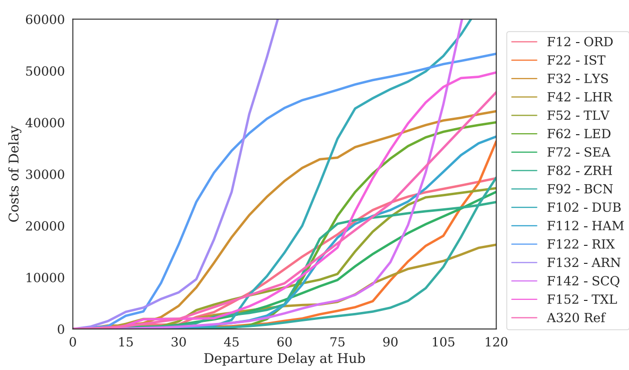

FIGURE 12. Stochastic delay cost function of all aircraft.

The planned capacity utilisation is marked by the green line in Fig. 13 and was retrieved from the initial flight plan data on Friday, 16 August 2019 – a day that did not contain any capacity regulations at Frankfurt airport. Based on this initial flight sequence, three constraint scenarios are introduced, which each predict the runway capacity to reduce to $AQ = 15$ while the length of the stress period varies. All scenarios assume that all flights will be operated, such that potential cancellations are neglected. The stress period is estimated to start before the morning peak at 7:00 a.m. local time. In Scenario 1 (S1), it is estimated to last for two hours, while in Scenario 2 (S2) it includes

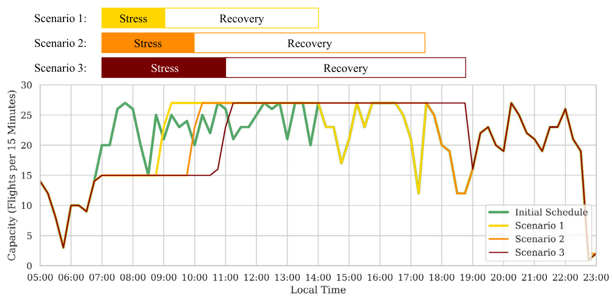

FIGURE 13. Airport constraint scenarios during the morning hub bank at Frankfurt airport.

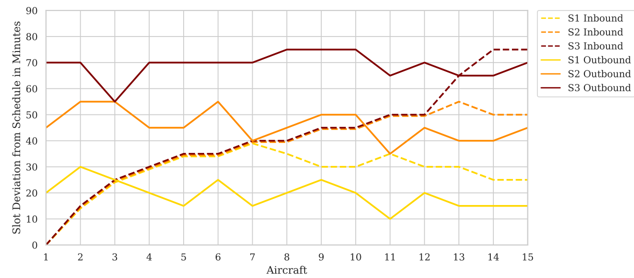

FIGURE 14. Assigned ATFCM delays per aircraft and scenario according to the RBS principle.

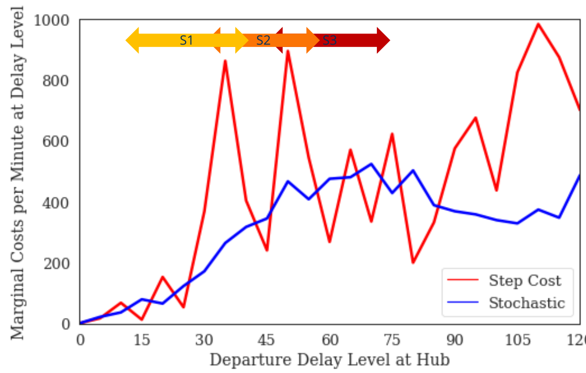

FIGURE 15. Comparison of marginal delay costs per minute across all flights within different types of delay cost functions.

three hours and in Scenario 3 (S3) four hours. As demand exceeds capacity during the entire stress period, slots are assigned according to the RBS principle. This results in a recovery period until 2:00 p.m. in S1 which also covers the entire midday bank. Given that more flights are affected by the stress period in S2, the recovery period covers almost the entire afternoon bank until 5:30 p.m. In S3, it lasts for another 75 minutes (see Fig. 13). Based on this initial slot assignment, the required arrival times and calculated take-off times per scenario are retrieved per flight of the case study airline and define sets of arrival slots AS and departure slots DS. Considering a typical cut-off time for the submission of flight priorities, which is two hours before the start of the constraint [2], we assume a look-ahead time of three hours before the problem, such that there is one hour left for the airline to define the priorities of their flights within their assigned slots. Each scenario is run with two instances, whereby the first one (S1/2/3-Step Cost) applies deterministic step cost functions, and in the second one (S1/2/3-Stochastic), stochastic cost functions are used to estimate the impact on downstream operations.

Fig. 14 exhibits the initially assigned delays to the arrival and departure flights of the same aircraft according to the RBS principle. Note that delays increase on flights early in the stress period, stagnate at the end of the stress period and begin to decrease once free capacity is available during the recovery period. Given the very heterogeneous ground times, which are typical for a full-service carrier, the available turnaround time between both slots is tighter for some aircraft than for others.

For example, in S1, almost all arrival flights receive higher delays than the respective departure flights of the same aircraft. Thereby, the flights of aircraft 7 and 11 obtain the largest difference (i.e., 25 minutes), which is critical for aircraft 7, due to no scheduled ground buffer, but uncritical for aircraft 11, which has 75 minutes ground buffer (see Fig. 7). In S2, aircraft 11 to 15 have diverging arrival and departure delays, whereas, in S3, only aircraft 14 and 15 are concerned. Thereby, aircraft 12 to 15 have very little to no absorption potential for arrival delays, given that their turnaround is scheduled for 45 and 50 minutes. Thus, both departure flights may require new departure slots, which are assumed to be available at 12:00 p.m. and 12:30 p.m.

V. ANALYSIS

The schedule recovery model was solved with IBM CPLEX Version 12.10.0-0 on a 4-core CPU with 32GB RAM. Results have been analysed with regard to airline costs (objective function), the underlying departure delay as the major driver for downstream costs and the required recovery options to achieve an optimal solution for the airline.

A. AIRLINE COSTS

Table 1 lists the resulting costs for all scenario instances, comparing them between a 'No Recovery' instance with a fixed slot assignment according to the RBS principle and a 'Schedule Recovery' instance, where additional turnaround resources are available and arrival as well as departure slots can be swapped among each other. In S1, the baseline 'No Recovery' estimation with step costs exceeds the stochastic one by only 500 EUR (+2%), while the offset increases to 67,000 EUR (+28%) in S3. As noted before in Section IV-C, the generally lower stochastic cost estimations can be related to the fact that stochastic cost functions are skewed along the delay axis due to increasing block and ground time uncertainties at higher look ahead times. Fig. 15 underlines this by comparing marginal costs per minute at different delay levels across all flights. Thus, the assigned ATFM delays in the 'No Recovery' instance cannot avoid extreme peaks in the step cost functions, which do not appear to this extend within the stochastic cost functions.

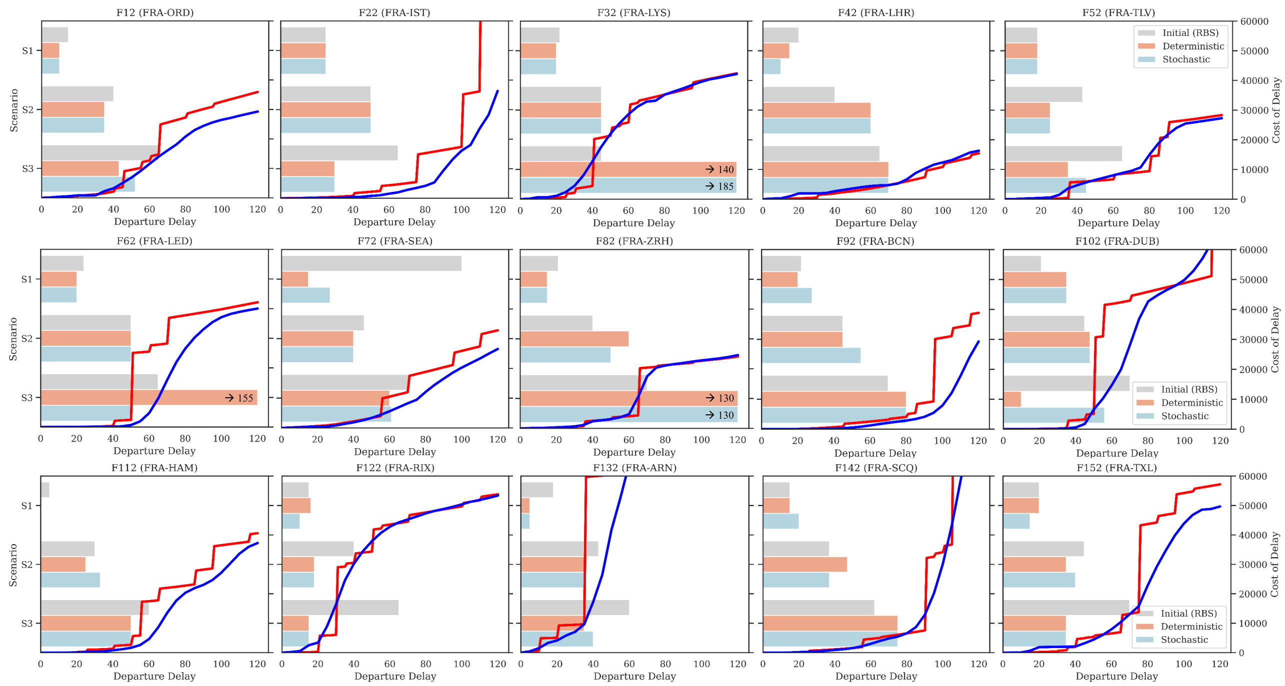

FIGURE 16. Assigned departure delay per flight in comparison to the delay cost functions.

Despite the different cost bases, the ratio of cost reductions through schedule recovery is similar with both types of functions in S1. However, the optimal recovery decisions to achieve such cost reductions differ when deterministic and stochastic cost functions are applied. With increasing delays in S2 and S3, the achieved cost savings with schedule recovery differ significantly between delay cost instances, such that the optimization based on deterministic costs scores the highest cost savings of up to 58%, though counted from a much higher baseline.

For a better comparative assessment, we evaluate another instance per scenario in which the optimal recovery decisions obtained with the step cost model are applied to the model with stochastic cost functions. In S1, this would result in 9,045 EUR, such that the optimal decisions based on deterministic step cost functions result in 52% higher cost. In S2, stochastic costs of deterministic optimal recovery decisions are 59,473 EUR. This is 2% above the optimal costs that could be achieve when considering stochastic costs in the recovery process. In S3, optimal recovery decisions based on deterministic costs would incur 167,691 EUR when evaluated with stochastic costs, which is 22,000 EUR (15%) higher than a schedule recovery based on stochastic costs.

B. OPTIMAL DEPARTURE DELAY

Fig. 16 shows the optimal departure delay per flight in comparison to the applied delay cost functions. It is obvious that the optimal delay (and slot) assignment very much mirrors the shape of the incorporated cost functions. Given that all cost functions are still closely aligned with each other at low delay levels, many of the assigned slots are similar or even equal between instances in S1 and S2. Thereby, the difference in the mean absolute deviation of optimal delays from the 'No Recovery' baseline is 1.3 minutes in S1 and 3.1 minutes in S2.

TABLE 1. Additional airline cost from airport constraints.

ID	Cost Function	No Recovery (RBS)	Schedule Recovery
S1	Step Cost	33,733	3,991 (-88%)
S1	Stochastic	33,210	5,960 (-82%)
S2	Step Cost	142,532	60,302 (-58%)
S2	Stochastic	95,136	58,042 (-39%)
S3	Step Cost	310,896	170,878 (-45%)
S3	Stochastic	243,322	145,492 (-40%)

Starting at delays above 45 minutes, the offset between both types of cost functions becomes more apparent, such that it causes a larger heterogeneity among optimal delay values per flight in S3. The mean absolute deviation of optimal delays from the baseline ranges from 30.3 minutes with step costs to 36.9 minutes with stochastic costs. Almost all departure flights are swapped to another slot for an optimal recovery solution, whereby 9 swaps are performed differently between deterministic and stochastic instances (see Table 2). Note how in the deterministic instances many delays are assigned directly before larger step costs (see flights F12, F52, F92, F112, F122, F132, F152 in Fig. 16). In comparison, stochastic cost functions consider downstream recovery potential and block time uncertainties, which smooths the cost functions and allows some flights to obtain departure delays slightly higher than a critical delay threshold – best visible at flights F12, F52, F102 and F132. This frees up time and resources which can be allocated to more critical

TABLE 2. Optimal number of applied schedule recovery options per scenario. Slot swap values in parenthesis mark the amount of differently assigned swaps between step cost and stochastic instances of the same scenario.

ID	Cost Function	# ARR Slot Swaps (Δ)	Quick-Turn	# DEP Slot Swaps (Δ)	# Misconnex
S1	Step Cost	4 (2)	Aircraft 7	5 (1)	6
S1	Stochastic	6 (4)	Aircraft 13	6 (2)	4
S2	Step Cost	5 (3)	Aircraft 13	6 (3)	6
S2	Stochastic	6 (4)	Aircraft 13	5 (2)	6
S3	Step Cost	8 (7)	Aircraft 13	12 (9)	15
S3	Stochastic	9 (8)	Aircraft 13	12 (9)	12

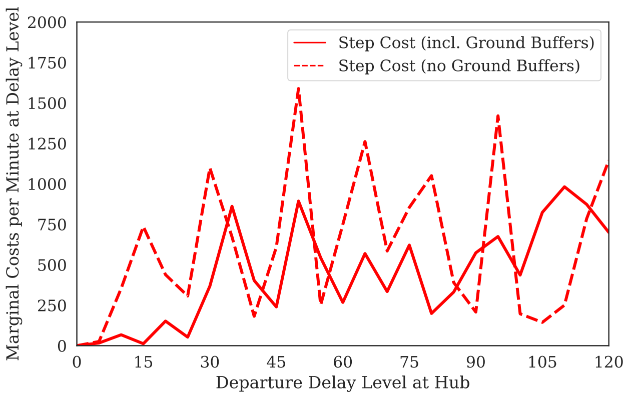

FIGURE 17. Potential change in marginal costs if the airline would schedule no ground buffers between the flights in each aircraft rotation.

aircraft rotations (e.g., flight F62 can be held in a slot before a downstream constraint that would incur more than 20,000 EUR).

C. SENSITIVITY OF OPTIMAL RECOVERY DECISIONS

As mentioned in Section V-A, different recovery decisions are required to achieve optimal solutions on the basis of deterministic and stochastic delay cost functions. Table 2 exhibits the optimal number of applied schedule recovery options per scenario instance. Note in S1 with low delays and deterministic step costs that the quick-turnaround procedure is assigned to wide-body aircraft 7 (F72) that would otherwise miss its initially assigned departure slot. Throughout all other instances, the quick-turnaround is assigned to aircraft 13 (F132) that is critical due to its scheduled maintenance event with only 35 minutes of buffer time and very high delay costs afterwards – which relate to a potential cancellation of the flight cycle to Stockholm (ARN). The optimal number of arrival and departure slot swaps increases with the magnitude of delay from S1 to S3. Thereby, also the number of differently performed swaps between instances of the same scenario (marked in parenthesis in Table 2) increases at higher delays. Finally, up to three passenger transfer connections can be maintained when stochastic delay cost functions are considered in the optimisation process. This might be related to the fact that stochastic cost functions are able to incorporate 'hidden' downstream recovery potential into local decision making, such that some aircraft can wait longer on stand for critical transfers.

VI. CONCLUSION

This article describes how flight-specific delay cost functions enable a detailed consideration of how a given primary delay may interact with downstream constraints and recovery potential within an airline network. When applying our methodology to an airline case study, we find that deterministic delay cost functions consistently overestimate the potential costs arising from a disruption. Compared to this, stochastic delay cost functions present a more realistic estimation of the costs that may be caused by delay propagation, given that they consider uncertainties in the system and reveal 'hidden' downstream recovery potential. This may benefit local schedule recovery and flight prioritization processes when airport resources are constrained. In the case study, optimal recovery decisions based on stochastic delay costs result in different slot allocations and include fewer missed passenger transfers at the hub airport. Thereby, decisions of the stochastic model outperform those generated on the basis of deterministic delay costs by up to 15% in a high delay scenario.

Note that the presented application in this article had the aim to validate the methodology, such that the findings need to be verified with a higher number of scenarios in future work. Thereby, it will be essential to have access to a comprehensive data base of historical operations data, such that stochastic cost estimations can be generated with conditional probabilities that are derived from larger data samples (especially for high delays). For the presented case study network, conditional probabilities of primary delays propagating along aircraft rotations are derived from open-access flight plan data of one season, while flight cancellation at higher delays have entirely been neglected.

Future research may also extend the scope of the researched disruption scenarios or apply delay cost functions to other types of airline planning models. Thereby, it might be worth investigating how the specific business model of an airline and the related network or recovery strategies influence the shape of its delay cost functions. Fig. 17 presents a sketched example in which all scheduled ground buffers have been omitted from the aircraft rotations in the airline case study network. It is clear that marginal delay costs increase at lower delay levels and accumulate to even higher peaks, given that the heterogeneity of aircraft ground times and, thus, also the available connecting times for transfer passengers, decrease.

Finally, further studies may assess the stability of optimal schedule recovery decisions when stochastic delay cost functions are applied. Given that step costs are smoothed due to block time variances, the associated constraints are less rigid. This may result in longer solution times which might require appropriate solution methods [64]. Besides, optimal decisions based on stochastic costs might be less stable when the duration of a capacity constraint or the related flight delays change due to prediction uncertainties [54], [65].

ACKNOWLEDGMENT

The opinions expressed herein reflect the authors' views only. Under no circumstances shall the SESAR Joint Undertaking be responsible for any use that may be made of the information contained herein.

REFERENCES

[1] M. Ball, C. Barnhart, G. Nemhauser, and A. Odoni, ''Air transportation: Irregular operations and control,'' in *Handbooks Operations Research and Management Science*, vol. 14. Cambridge, MA, USA: Elsevier, 2007, pp. 1–67.

[2] N. Pilon, A. Cook, S. Ruiz, A. Bujor, and L. Castelli, ''Improved flexibility and equity for airspace users during demand-capacity imbalance,'' in *Proc. 6th SESAR Innov. Days*, Delft, The Netherlands, 2016, p. 8.

[3] A. J. M. Castro and E. Oliveira, ''A new concept for disruption management in airline operations control,'' *Proc. Inst. Mech. Eng., G, J. Aerosp. Eng.*, vol. 225, no. 3, pp. 269–290, Mar. 2011.

[4] J. D. Petersen, G. Sölveling, J. P. Clarke, E. L. Johnson, and S. Shebalov, ''An optimization approach to airline integrated recovery,'' *Transp. Sci.*, vol. 46, no. 4, pp. 482–500, Nov. 2012.

[5] J. Evler, E. Asadi, H. Preis, and H. Fricke, ''Airline ground operations: Schedule recovery optimization approach with constrained resources,'' *Transp. Res. C, Emerg. Technol.*, vol. 128, Jul. 2021, Art. no. 103129.

[6] *PRR 2019–Performance Review Report*, EUROCONTROL, Brussels, Brussels, Belgium, vol. 2020.

[7] A. Cook and G. Tanner, ''European airline delay cost reference values: Updated and extended values,'' Univ. Westminster, London, U.K., Tech. Rep. 4.1, 2015.

[8] R. Beatty, R. Hsu, L. Berry, and J. Rome, ''Preliminary evaluation of flight delay propagation through an airline schedule,'' *Air Traffic Control Quart.*, vol. 7, no. 4, pp. 259–270, Oct. 1999.

[9] S. AhmadBeygi, A. Cohn, Y. Guan, and P. Belobaba, ''Analysis of the potential for delay propagation in passenger airline networks,'' *J. Air Transp. Manage.*, vol. 14, no. 5, pp. 221–236, Sep. 2008.

[10] C.-L. Wu and K. Law, ''Modelling the delay propagation effects of multiple resource connections in an airline network using a Bayesian network model,'' *Transp. Res. E: Logistics Transp. Rev.*, vol. 122, pp. 62–77, Feb. 2019.

[11] L. Carvalho, A. Sternberg, L. Maia Gonçalves, A. Beatriz Cruz, J. A. Soares, D. Brandão, D. Carvalho, and E. Ogasawara, ''On the relevance of data science for flight delay research: A systematic review,'' *Transp. Rev.*, vol. 41, no. 4, pp. 499–528, Jul. 2021.

[12] C.-L. Wu, *Airline Operations and Delay Management: Insights from Airline Economics, Networks and Strategic Schedule Planning*. Evanston, IL, USA: Routledge, Mar. 2016.

[13] *A320–Aircraft Characteristics Airport and Maintenance Planning*, Airbus, Leiden, The Netherlands, 2020.

[14] T. Bieger and A. Wittmer, ''Airline strategy: From network management to business models,'' in *Aviation Systems*. St. Gallen, Switzerland: Springer, 2011, pp. 77–102.

[15] G. Gurtner and A. Cook, ''The hidden cost of uncertainty for airspace users,'' *J. Air Transp. Manage.*, vol. 91, Mar. 2021, Art. no. 102002.

[16] C.-L. Wu, ''Improving airline network robustness and operational reliability by sequential optimisation algorithms,'' *Netw. Spatial Econ.*, vol. 6, nos. 3–4, pp. 235–251, Sep. 2006.

[17] S. AhmadBeygi, A. Cohn, and M. Lapp, ''Decreasing airline delay propagation by re-allocating scheduled slack,'' *IIE Trans.*, vol. 42, no. 7, pp. 478–489, Apr. 2010.

[18] J. M. Rosenberger, A. J. Schaefer, D. Goldsman, E. L. Johnson, A. J. Kleywegt, and G. L. Nemhauser, ''A stochastic model of airline operations,'' *Transp. Sci.*, vol. 36, no. 4, pp. 357–377, 2002.

[19] M. A. Aloulou, M. Haouari, and F. Zeghal Mansour, ''A model for enhancing robustness of aircraft and passenger connections,'' *Transp. Res. C, Emerg. Technol.*, vol. 32, pp. 48–60, Jul. 2013.

[20] M. Dunbar, G. Froyland, and C.-L. Wu, ''An integrated scenario-based approach for robust aircraft routing, crew pairing and re-timing,'' *Comput. Oper. Res.*, vol. 45, pp. 68–86, May 2014.

[21] L. Marla, V. Vaze, and C. Barnhart, ''Robust optimization: Lessons learned from aircraft routing,'' *Comput. Oper. Res.*, vol. 98, pp. 165–184, Oct. 2018.

[22] J. M. Rosenberger, E. L. Johnson, and G. L. Nemhauser, ''A robust fleet-assignment model with hub isolation and short cycles,'' *Transp. Sci.*, vol. 38, no. 3, pp. 357–368, Aug. 2004.

[23] L. S. Kang, ''Degradable airline scheduling: An approach to improve operational robustness and differentiate service quality,'' Ph.D. dissertation, Massachusetts Inst. Technol., Cambridge, MA, USA, 2004.

[24] A. Cook, G. Tanner, S. Cristobal, and M. Zanin, ''Delay propagation–new metrics, new insights,'' in *Proc. 11th USA/Eur. Air Traffic Manage. Res. Develop. Seminar (ATM)*, 2015, p. 11.

[25] A. J. Cook, G. Tanner, S. Cristóbal, and M. Zanin, ''New perspectives for air transport performance,'' in *Proc. 3rd SESAR Innov. Days*, Stockholm, Sweden, 2013, p. 9.

[26] European Union, *Regulation (EC)*, document 261/2004, 2004.

[27] J. Clausen, A. Larsen, J. Larsen, and N. J. Rezanova, ''Disruption management in the airline industry—Concepts, models and methods,'' *Comput. Oper. Res.*, vol. 37, no. 5, pp. 809–821, May 2010.

[28] L. K. Hassan, B. F. Santos, and J. Vink, ''Airline disruption management: A literature review and practical challenges,'' *Comput. Oper. Res.*, vol. 127, Mar. 2021, Art. no. 105137.

[29] L. Lettovsky, ''Airline operations recovery: An optimization approach,'' Ph.D. dissertation, Oper. Res. Center, MIT, Cambridge, MA, USA, 1997.

[30] S. Bratu and C. Barnhart, ''Flight operations recovery: New approaches considering passenger recovery,'' *J. Scheduling*, vol. 9, no. 3, pp. 279–298, Jun. 2006.

[31] N. Kohl, A. Larsen, J. Larsen, A. Ross, and S. Tiourine, ''Airline disruption management—Perspectives, experiences and outlook,'' *J. Air Transp. Manage.*, vol. 13, no. 3, pp. 149–162, May 2007.

[32] J. Vink, B. F. Santos, W. J. C. Verhagen, I. Medeiros, and R. Filho, ''Dynamic aircraft recovery problem–An operational decision support framework,'' *Comput. Oper. Res.*, vol. 117, May 2020, Art. no. 104892.

[33] J. Lee, L. Marla, and A. Jacquillat, ''Dynamic disruption management in airline networks under airport operating uncertainty,'' *Transp. Sci.*, vol. 54, no. 4, p. 26, 2020.

[34] A. Cook, G. Tanner, V. Williams, and G. Meise, ''Dynamic cost indexing–managing airline delay costs,'' *J. Air Transp. Manage.*, vol. 15, no. 1, pp. 26–35, Jan. 2009.

[35] L. Delgado, J. Martin, A. Blanch, and S. Cristobal, ''Hub operations delay recovery based on cost optimisation,'' in *Proc. 6th SESAR Innov. Days*, Delft, The Netherlands, 2016, p. 11.

[36] U. Arikan, S. Gürel, and M. S. Aktüürk, ''Integrated aircraft and passenger recovery with cruise time controllability,'' *Ann. Oper. Res.*, vol. 236, no. 2, pp. 295–317, Jan. 2016.

[37] L. Marla, B. Vaaben, and C. Barnhart, ''Integrated disruption management and flight planning to trade off delays and fuel burn,'' *Transp. Sci.*, vol. 51, no. 1, pp. 88–111, Feb. 2017.

[38] J. Rosenow and M. Schultz, ''Coupling of turnaround and trajectory optimization based on delay cost,'' in *Proc. Winter Simul. Conf. (WSC)*, Gothenburg, Sweden, Dec. 2018, pp. 2273–2284.

[39] J. Kuster, D. Jannach, and G. Friedrich, ''Extending the RCPSP for modeling and solving disruption management problems,'' *Int. J. Speech Technol.*, vol. 31, no. 3, pp. 234–253, Dec. 2009.

[40] B. Oreschko, T. Kunze, M. Schultz, H. Fricke, V. Kumar, and L. Sherry, ''Turnaround prediction with stochastic process times and airport specific delay pattern,'' in *Proc. 5th Int. Conf. Res. Air Transp. (ICRAT)*, Jun. 2012, p. 9.

[41] M. Schultz, B. Oreschko, H. Fricke, and T. Kunze, ''Microscopic process modelling for efficient aircraft turnaround management,'' in *Proc. 4th Int. Air Transp. Oper. Symp.*, Delft, Jul. 2013, p. 12.

[42] M. Abd Allah Makhloof, M. Elsayed Waheed, and U. A. El-Raouf Badawi, ''Real-time aircraft turnaround operations manager,'' *Prod. Planning Control*, vol. 25, no. 1, pp. 2–25, Jan. 2014.

[43] J. Evler, E. Asadi, H. Preis, and H. Fricke, ''Stochastic control of turnarounds at HUB-airports,'' in *Proc. 8th SESAR Innov. Days*, Salzburg, Austria, 2018, p. 9.

[44] M. Tomasella, A. Clare, Y. S. Gok, D. Guimarans, and C. Ozturk, ''Sttar: A simheuristics-enabled scheme for multi-stakeholder coordination of aircraft turnaround operations,'' in *Proc. Winter Simulation Conf. (WSC)*, Dec. 2019, pp. 488–499.

[45] H. Fricke and M. Schultz, ''Delay impacts onto turnaround performance,'' in *Proc. 8th USA/Eur. Air Traffic Manage. Res. Develop. Seminar (ATM)*, 2009, p. 10.

[46] A. Montlaur and L. Delgado, ''Flight and passenger delay assignment optimization strategies,'' *Transp. Res. Part C: Emerg. Technol.*, vol. 81, pp. 99–117, Aug. 2017.

[47] B. F. Santos, M. M. E. C. Wormer, T. A. O. Achola, and R. Curran, ''Airline delay management problem with airport capacity constraints and priority decisions,'' *J. Air Transp. Manage.*, vol. 63, pp. 34–44, Aug. 2017.

[48] A. Cook, G. Tanner, and T. Bolic, "SESAR beacon D3.2–industry briefing on updates to the European cost of delay," Univ. Westminster, London, U.K., Tech. Rep. D3.2, 2021.
[49] European Union, *Regulation (EC)*, document 83/2014, 2014.
[50] L. Delgado, A. Blanch, S. Cristobal, and J. Martin, "CASSIOPEIA II D3. 2-final technical report," Univ. Westminster, London, U.K., Tech. Rep. D3, 2016.
[51] S. Ruiz, L. Guichard, and N. Pilon, "Optimal delay allocation under high flexibility conditions during demand-capacity imbalance," in *Proc. 7th SESAR Innov. Days*, Belgrade, Serbia, 2017, p. 28.
[52] N. Pilon, K.-D. Hermann, A. Ds, P. Hlousek, M. Hripane, E. P. Parla, F. Rousseau, D. Chiesa, G. Q. Albert, and D. Müller, "PJ07 final project report," EUROCONTROL, Brussels, Belgium, Tech. Rep. D1.2, 2019.
[53] Y. Guleria, Q. Cai, S. Alam, and L. Li, "A multi-agent approach for reactionary delay prediction of flights," *IEEE Access*, vol. 7, pp. 181565–181579, 2019.
[54] J. Evler, M. Schultz, H. Fricke, and A. Cook, "Development of stochastic delay cost functions," in *Proc. 10th SESAR Innov. Days*, 2020, p. 9.
[55] M. F. Yazdi, S. R. Kamel, S. J. M. Chabok, and M. Kheirabadi, "Flight delay prediction based on deep learning and levenberg-marquart algorithm," *J. Big Data*, vol. 7, no. 1, pp. 1–28, Dec. 2020.
[56] R. Dalmau, B. Genestier, C. Anoraud, P. Choroba, and D. Smith, "A machine learning approach to predict the evolution of air traffic flow management delay," in *14th ATM Res. Develop. Seminar*, 2021, p. 8.
[57] A. Cook and G. Tanner, "The cost of passenger delay to airlines in Europe," Univ. Westminster, London, U.K., Tech. Rep. 2.0, 2015.
[58] C. Wu and R. E. Caves, "Modelling and optimization of aircraft turnaround time at an airport," *Transp. Planning Technol.*, vol. 27, no. 1, pp. 47–66, Feb. 2004.
[59] M. Schultz, "Implementation and application of a stochastic aircraft boarding model," *Transp. Res. C, Emerg. Technol.*, vol. 90, pp. 334–349, May 2018.
[60] C. E. Miller, A. W. Tucker, and R. A. Zemlin, "Integer programming formulation of traveling salesman problems," *J. ACM*, vol. 7, no. 4, pp. 326–329, 1960.
[61] M. Schultz, S. Lorenz, R. Schmitz, and L. Delgado, "Weather impact on airport performance," *Aerospace*, vol. 5, no. 4, p. 109, Oct. 2018.
[62] J. Evler, "Resource-constrained airline ground operations: Optimising airline schedule recovery under uncertainty," Ph.D. dissertation, Oper. Res. Center, MIT, Cambridge, MA, USA, 2022.
[63] "Dynamic cost indexing technical discussion document 5.0 aircraft crewing–marginal delay costs," Univ. Westminster, London, U.K., Tech. Rep. 5.0, 2008.
[64] P. Manyem, "A note on optimization modelling of piecewise linear delay costing in the airline industry," *J. Ind. Manage. Optim.*, vol. 17, no. 4, p. 1809, 2021.
[65] J. Evler, E. Asadi, H. Preis, and H. Fricke, "Airline ground operations: Optimal schedule recovery with uncertain arrival times," *J. Air Transp. Manage.*, vol. 92, May 2021, Art. no. 102021.

JAN EVLER received the B.Sc. degree in industrial engineering and management from Technische Universität (TU) Dresden, in 2015, and the master's degree in transport economics from the University of Lugano, Switzerland, in 2017. He is currently pursuing the Ph.D. degree in transport engineering with the Institute of Logistics and Aviation, TU Dresden. Since 2018, he has been a Research Associate with the Institute of Logistics and Aviation, TU Dresden. His Ph.D. studies are supported and partially funded by the Scholarship from the SESAR Knowledge Transfer Network, Engage. His research interests include airline operations research, resource-constrained process scheduling, and delay propagation in transport networks.

MICHAEL SCHULTZ received the Diploma degree in business and engineering, the Ph.D. degree in logistics and aviation technologies, and the Habilitation degree in aviation from Technische Universität (TU) Dresden, Germany, in 2002, 2010, and 2019, respectively. From 2014 to 2019, he was the Head of the Air Transportation Department, German Aerospace Center (DLR e.V.). Since 2019, he has been a Senior Principal Researcher with the Institute of Logistics and Aviation, TU Dresden; and a Visiting Researcher with the Air Traffic Management Research Institute, Nanyang Technological University, Singapore. His research interests include data-driven and model-based approaches to improve air transportation, flow-centric airspace management, inter-airport coordination, performance-based airport and aircraft operations, and advanced concepts for future traffic management. He is an Editorial Board Member of *Transportation Research—C: Emerging Technologies* and the Section Editor-in-Chief of *Air Traffic and Transportation* and a section of *Aerospace*.

HARTMUT FRICKE studied aeronautics and astronautics at Technische Universität (TU) Berlin, from 1985 to 1991. From 1991 to 1995, he was a Research Fellow in flight operations, airport planning, and air traffic management (ATM) with TU Berlin, where he completed his doctoral thesis in ATM. In 2001, he finished his Habilitation on Integrated Collision Risk Modeling for Airborne and Ground-Based Systems. This included human-in-the-loop experiments with an A340 full flight simulator in co-operation with the EUROCONTROL Experimental Center. Since December 2001, he has been the Head of the Institute of Logistics and Aviation and a Professor for aviation technologies and logistics with TU Dresden. In 2006, he was appointed as a member of the Scientific Advisory "Board of Advisors" to the Federal Minister of Transport, Building and Urban Affairs, Germany, which he led from 2018 to 2020. From 2014 to 2018, he was an Elected Member of the Expert Council for Systems Engineering of the German Research Foundation (DFG).

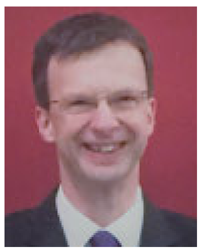

ANDREW COOK received the B.A. degree (Hons.) in natural sciences and the D.Phil. degree in physiological sciences (Sub-Faculty of Medical Sciences) from the University of Oxford, in 1989 and 1992, respectively. He subsequently joined the Transport Studies Unit, University of Oxford, as a Research Associate, before moving to the University of Westminster, London, where he currently leads the Air Traffic Management Team and was awarded the Full Professorship, in 2018. He has been leading work on approximately 30 major European ATM research projects, since 1999, mostly as a Project Coordinator: primarily funded through SESAR, EUROCONTROL, and the European Commission, and carried out in collaboration with airlines, airports, ANSPs, software/service providers, and other research institutes. Commercial work has been undertaken in cooperation primarily with universities, airlines, ANSPs, and numerous industry partners. He has acted as an Economic Advisor and a Scientific Evaluator for industry and national government. He is the Coordinator of the SESAR Knowledge Transfer Network, Engage; and a member of inter alia, the SESAR Scientific Committee, AGIFORS, ASDA, EUROCONTROL's ART, and the Programme Committee of the SESAR Innovation Days.